Smart Materials and Structures

TOPICAL REVIEW

Progress of shape memory polymers and their composites in aerospace applications

To cite this article: Fengfeng Li *et al* 2019 *Smart Mater. Struct.* **28** 103003

Smart Mater. Struct. 28 (2019) 103003 (23pp)
https://doi.org/10.1088/1361-665X/ab3d5f

Topical Review

Progress of shape memory polymers and their composites in aerospace applications

Fengfeng Li[1], **Yanju Liu**[1,3] and **Jinsong Leng**[2,3]

[1] Department of Astronautical Science and Mechanics, Harbin Institute of Technology (HIT), PO Box 301, No. 92 West Dazhi Street, Harbin 150001, People's Republic of China
[2] Centre for Composite Materials, Science Park of Harbin Institute of Technology (HIT), PO Box 3011, No. 2 YiKuang Street, Harbin 150080, People's Republic of China

E-mail: yj_liu@hit.edu.cn and lengjs@hit.edu.cn

Received 2 March 2019, revised 21 May 2019
Accepted for publication 21 August 2019
Published 23 September 2019

Abstract
Shape memory polymers and their composites are kind of smart materials, which can transfer from the temporarily fixed configuration to the original configuration under external stimuli. Their inherent advantages are low density, low cost, large recoverable deformation ability and controllable stimulus method, which make them an alternative for aerospace applications (deployable structures, release devices, wrinkled/slack control component, etc). Most of these applications are in development stage, some have completed the ground functional verification experiments, a rare part has been carried out the spaceflight experiments. This review focuses on their materials and structures in aerospace field, briefly introduces the development history and general mechanism of shape memory polymers and their composites, replenishes the space radiation resistance abilities of these materials under the ground-simulated space radiation experiments, tracks those applications who have already completed the spaceflight experiments, then exhibits some novel applications which have great potential and could give us inspirations for new aerospace application development, finally the prospects for materials and structures are discussed in the future outlook.

Keywords: shape memory polymer, shape memory polymer composite, space radiation, spaceflight experiment, potential application

(Some figures may appear in colour only in the online journal)

1. Introduction

Smart materials can sense, judge and respond to external stimuli, they incorporate the capabilities of sensing, driving, and controlling together. The developments of those materials, including shape memory ceramics (SMCs), shape memory alloys (SMAs) and shape memory polymers (SMPs), etc, have been underway for decades [1–3]. Particularly, SMPs represent a type of macro-molecular polymers which can switch from a temporarily fixed configuration to the original configuration under certain stimuli (heat [4–8], electricity [9–13], magnetism [14, 15], light [16–18], solution [19–23], etc). Schematics of shape recovery processes are shown in figure 1. Their inherent advantages are low density, low cost, large recoverable strain, controllable stimulus method, and flexible manufacturability of the glass transition temperature. The main drawbacks of SMPs are lower recovery stress (with the order of magnitude 10 MPa), smaller energy output (with the order of magnitude 10^{-1}–10^{0} MJ m^{-3}), longer recovery time (with the order of magnitude 10 s), and shorter cycle life (with the order of magnitude 10^{2}) compared to SMAs [24–27]. However, some drawbacks of SMPs could be translated into advantages in specific situations, for example, the long recovery time could result in small impact response

[3] Authors to whom any correspondence should be addressed.

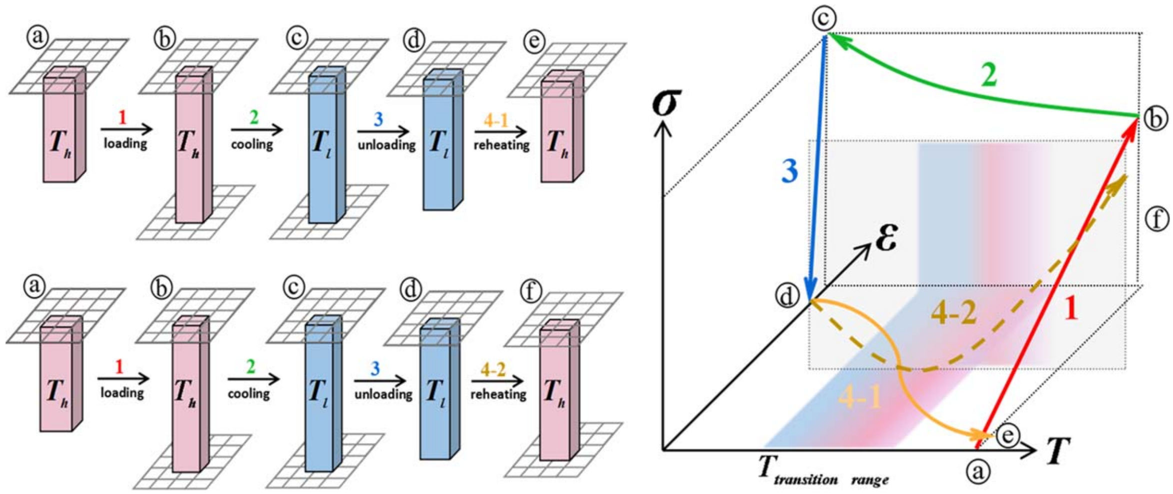

Figure 1. Schematics of shape recovery processes, (a) free recovery process, (b) constraint recovery process, (c) the temperature-strain–stress curves at different recovery process (1. Loading at high temperature (above Tg), 2. Cooling with external constraints, 3. releasing the constraints, 4–1 free recovery process, 4–2 constraint recovery process).

in release devices [28]. While the low recovery stress does limit the application of SMPs. Consequently, the shape memory polymer composites (SMPCs) have been developed to satisfy demands in various applications. They are generally divided into particles-reinforced and fiber-reinforced composites according to the type of reinforcements [2, 29–33]. Particles-reinforced SMPCs, whose fillers include Ni powders [9, 10], carbon black [21, 22], carbon nanotubes [34, 35], Fe3O4 nanoparticles [36], etc are more used as functional materials [9, 10, 21, 22, 34–37]. Fiber-reinforced SMPCs, whose fillers include carbon fibers [26, 38–40], glass fibers [27, 41] and Kevlar fibers [41], etc are usually used as structural materials due to their good mechanical properties [2, 26, 27, 38–41]. Studies on SMPCs indicate that they have relatively high strength, large recovery force, and high damping etc. They could be utilized in various applications, such as textiles [42–45], microelectronics [46–48], bio-medical [49], and aerospace [50, 51], etc.

Since the first literature mentioning shape memory effect of a methacrylic acid ester resin in 1941 [52, 53], it was not until the 1960s that SMPs had the first large-scale application when the covalently crosslinked polyethylene was made into thermal contraction tubes [53–56]. Tremendous endeavors started in the late 1980s where researchers' efforts were mainly focused on material synthesis [26, 57, 58]. During the 2000s, substantial applications in aerospace, biomedical have emerged and motivated the continuous study of material synthesis and characterization. Several typical SMPs have been commercialized, including polyurethane [27, 59], aliphatic polyurethane [60], polystyrene based SMP [61, 62], epoxy and cyanate based SMP [37, 63–65], polypropylene and polyester based SMP [66], etc. Meanwhile, several groups have been dedicated to the development of SMPs with specific properties for certain requirements, Osada for hydrogels [67–69], L Santo for foams and composites [70, 71], A Lendlein for biopolymers and medical devices [4, 18, 72–75], Hu for textiles and apparels [76–78], and Leng for thermoset SMPs and aerospace applications [51, 79–82]. Table 1 lists the potential SMPs for aerospace applications.

Table 1. Partial list of SMPs for potential aerospace alternatives.

Research group	SMP matrix	Glass transition temperature (°C)
SMP Technologies Inc.	Polyurethane [27, 59]	−40∼90
Lubrizol Advanced Materials	Aliphatic polyurethane [60]	74
Cornerstone Research Group, Inc.	Polystyrene [61]	45–106
	Epoxy based [62]	105
	Cyanate Ester [61]	135–230
Composite Technology Development, Inc.	Epoxy [37, 64]	79.3, 71
	Cyanate Ester [64]	155, 164, 170
ILC Dover, Inc.	Polyurethane [66]	55,75
	Epoxy [66]	48, 53, 65
	Polyester [66]	80
	Polypropylene [66]	80, 95, 108
3 M Company	Epoxy [70]	106
Leng's Group	Epoxy [81]	37–96
	Cyanate–ester [79]	156.9–256.9
	Polyimide [8]	321–323

To date, several excellent reviews, focusing on the SMP/SMPC syntheses, properties, simulation methods, applications, have been published [26, 51, 83–86]. We need to mention two previous reviews about the SMP/SMPC in aerospace filed. In 2001, Lake *et al* revealed the development of elastic memory composites (EMCs, namely carbon fiber reinforced SMPCs). The theoretical model, material evaluation, and applications there promoted other researchers to realize the practicability of SMPCs in aerospace applications [83]. In 2013, Liu *et al* reviewed the SMPs and SMPCs in aerospace applications from the mechanism, stimulus method to structures; detailed progresses of SMPC hinges, booms,

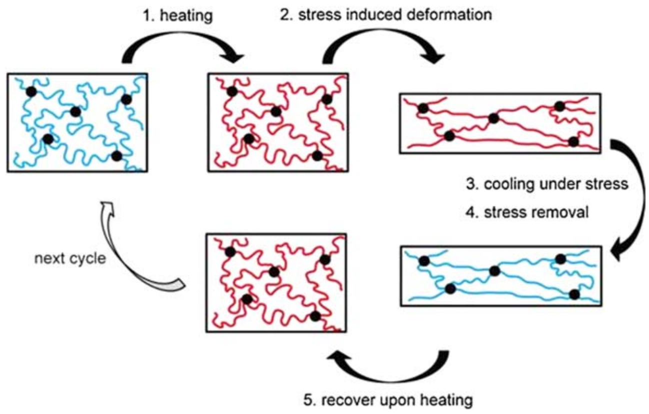

Figure 2. The molecular mechanism of the SMP, • crosslinking points; low mobility molecular chains below Tm/Tg; high mobility molecular chains above Tm/Tg [94].

solar array, reflector antenna, and morphing wing, etc [51]. This review focuses on the SMP/SMPC materials and structures in aerospace field, with aims of replenishing the material space radiation resistance capabilities found in open literature, tracking the applications who have already completed the spaceflight experiments, and listing new developed applications who are potential for the aerospace but at principle prototype stages.

2. General mechanism of SMP and SMPC

2.1. General mechanism of SMP

Shape memory property, the most distinguished property of SMP/SMPC, has been introduced in the previous review [51]. From the high polymer physics view, all polymeric materials possess the shape memory property substantially, just differ in recovery time. Some are too short, like the rubber would immediately have the elastic recovery once the external constraint is released; while others, like the deformed plastic which would take hundreds of or even thousands of years to have a small recovery. General polymers are covalently or physically cross-linked, exhibiting viscoelastic to large strain above either Tm (crystalline polymers) or Tg (amorphous polymers), and elastic to small strain at low temperature (figure 2). At the temperature above Tm/Tg, the polymer chain segments between the crosslinking points prone to deform freely, and twist randomly around the skeleton bond, thus keeping a maximum entropy and a minimum internal energy under macroscopic deformation [87]. The deformation usually happens at the temperature above Tm/Tg, where the flexible chain segments of the polymer are elongated or flowed along the deformation direction by external forces. During temperature decreasing, the movements of the chain segments are locked through networks' crystallization or vitrification, resulting in the material in a low energy state. The temporarily fixed configuration would be got after releasing the external constraint where the material is generally elastic at macroscopic, and there usually has an elastic shrink due to the segments' structural recoil. At the molecular level, either stress or strain would relax depending on the time, temperature, etc, the temporarily fixed configuration is actually in a non-equilibrium state but relatively stable for SMP/SMPC. Upon subsequent reheating to the temperature above Tm/Tg, the segments are unlocked, restoring to their most disordered conformation, thus the material recovery to its original configuration at macroscopic. The shape memory mechanism mentioned above inspires us that the fundamental prerequisites for polymers with significant shape memory property include: (1) successful accomplishment of shape programming by locking the polymeric segments without creep; (2) a sharp transition of the modulus corresponding to temperature, which would promptly lead to a temporarily fixed shape at low temperature and stimulate shape recovery at high temperature; (3) viscoelasticity above Tm/Tg that ensure a relatively complete shape recovery without residual strain [76, 88–93].

The constitutive models of SMP could be categorized into two sections: thermoviscoelastic modeling approaches and phase transition modeling approaches [95]. Materials in the thermoviscoelastic model are often assumed as combinations of springs, dashpots and frictional elements, the representative works are Tobushi model [96, 97], Nguyen model [98], Gu model [99], etc. These models are suitable to describe rate-dependent behavior on macroscopic level [2]. The phase transition models are migrated from the SMA's model, dividing the material basically into active and frozen phases [100–102]. It is phenomenological for amorphous SMPs, but can find physical meaning in semicrystalline SMPs. Representative works are Liu model [100], Chen and Lagoudas model [101, 102]. Some researchers integrated the two approaches together, describing the mechanical behavior of the individual phase with viscoelasticity equations [103–105].

2.2. General mechanism of SMPC

The low mechanical properties of SMPs are limiting factors for their commercial applicability. Consequently, SMPCs have been developed. Usually, the reinforcement ability of continuous fiber is the highest, followed by the short fibers and the particles. To date, the open literature about the SMPCs for aerospace application is primarily continuous fiber reinforced SMPCs, normally carbon fiber or fabric since their high reinforcement, good physical and chemical properties. Though the maximum elongation ratio of carbon fibers is less than 2%, restricting the tensile deformation of SMPCs [64, 106–112]. These continuous fiber reinforced SMPCs could survive under large macro bending deformation. Researchers have put tremendous efforts to explore the bending mechanism of SMPCs, and concluded the micro-buckling is the reason (figure 3). Micro-buckling happens at large bending ratio when a fibre reinforced SMPC is heated to the temperature above Tm/Tg. At this situation, the SMP matrix has a low shear modulus (with the order of magnitude 10 MPa), and does not have enough stiffness to support those fibers in compression. Consequently, those fibers would have micro-buckling as a result of instability. This enables a

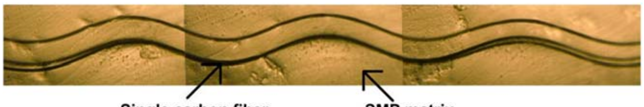

Figure 3. The post-microbuckling of fiber reinforced SMPC under compressive loading [113].

relatively large fiber compression strain since the buckled fiber appears shorter than that of the unbuckled one in macro scale. The amplitude of the micro buckle is the place to accommodate the change in length. The macro strain of the buckled SMPC is above the conventional material strain failure limit. While, it should be noted that the thickness of the SMPC is usually less than 2 mm, since a thicker laminate or a laminate with large modulus would have a large shear force to prevent the bending of fibers or damage the matrix.

In the 1750s, Euler investigated the characteristic deformation, buckling, of a rod under the axial load, and derived the Euler formula to calculate the load-bearing ability of the rod [114]. Euler's work is the fundamental of the following study. Since 1999, the Composite Technology Development Inc., Lafayette, CO (CTD) has been developing the SMPs and their fiber/fabric reinforced composites (namely EMC), and led the way to study the micro-mechanisms deformation of EMC [83, 115–117]. Lan *et al* and Zhang *et al* have followed the micro-buckling study of unidirectional carbon fiber reinforced SMPC, experimental and analytical studied the critical buckling position, the neutral plane, the amplitude and the half-wavelength of the buckled fiber by using strain energy method [113, 118]. Some researchers combined the theoretical models of SMPs and rule of mixture of composites to describe the thermomechanical behavior of SMPCs [119–121].

3. Effects of space environment on SMP/SMPC

The selection of new material for aerospace usage requires evaluations of performance under various ground simulated space radiations. Space radiations, including high vacuum, thermal cycling, ultraviolet radiation (UV), atomic oxygen (AO), plasma environment (ions and electrons), space debris, etc, can cause degradation of material, induce damage of component or structure, reduce system's reliability, and even shorten spacecraft's service life [122–130]. After years of investigation, researchers have found that the high vacuum, thermal cycling, UV, and AO are harsh space environmental factors, which have significant effects on materials [65, 131–146]. Therefore, this section will review the impacts of the above four space radiations on SMP/SMPC performances, exploring the mechanism of radiation damage in order to adopt appropriate protective methods to elongate the material life.

3.1. High vacuum

The high vacuum environment can cause material degassing, sublimation, mass loss, and even changes in physical and dielectric properties. When vacuum level reaches about 10^{-2} Pa, the gas adsorbed on the surface or dissolved in the material could be detached and released. If the released gas condenses or deposit on the surface of devices, such as an optical instrument, the device will be contaminated. In addition, the high vacuum may also induce space charge which might result in short-circuit or breakdown of instruments, and cold welding of materials which might obstruct moving parts. There is a standard test method ASTM E595 for evaluating the material performance in the high vacuum environment. Though different materials have different mass losses in the vacuum environment. Generally, aerospace materials require total mass loss (TML) in vacuum environment not exceeding 1.00%, collected condensable volatiles matter (CVCM) no more than 0.1% [64, 65, 131, 133].

Table 2. Vaccum-outgas experimental results of relevant materials [65, 142].

Material	Tg, °C	TML, %	CVCM, %
Tembo® DP5.1	71	0.87%	<0.01%
Tembo® 5XQ	77	0.90%	0.03%
Tembo® BG1.3	164	0.32%	0.03%
SMP-CRIV	205	1.04%	0.01%

The CTD has developed Tembo® EMC materials for years. As we mentioned above, EMC is another saying about SMPC, it is widely used in literature by CTD or Air Force Research Laboratory. In order to promote the application of EMC in aerospace field, CTD has conducted vacuum-outgas experiments of Tembo® series materials (Tembo® DP5.1, Tembo® 5XQ, Tembo® BG1.3, corresponding to epoxy, epoxy and cyanate esters matrix respectively) around 2000 [65]. They all passed the requirements that TML no more than 1.0% and CVCM no more than 0.1%. Results are shown in table 2. Leng's group also carried out vacuum-outgas experiments on cyanate-based SMP (Tg 205 °C), marked as SMP-CRIV in the following, according to the ASTM E595 standard. The TML, CVCM and collected water vapor were 1.04%, 0.01% and 0.80% respectively. The TML exceeded the upper limit of 0.04%, but the CVCM met the requirement of less than 0.1% [142]. Since most of the mass loss of SMP-CRIV is water vapor, which would not deposit significantly on optoelectronic components' surfaces. This material can still be considered as a candidate for aerospace-grade material. But when such materials are actually used in the aerospace field, they should better be degassed or deflated before usage.

3.2. Thermal cycling

The thermal cycling experiment is a basic and routine test for anything that targets on spaceflight since every spacecraft experiences large temperature difference in orbit. There are two reasons for the temperature difference. One is the difference between the illuminated surface and the non-illuminated surface, and the other is the alternate temperature change caused by the alternately move in and out of the

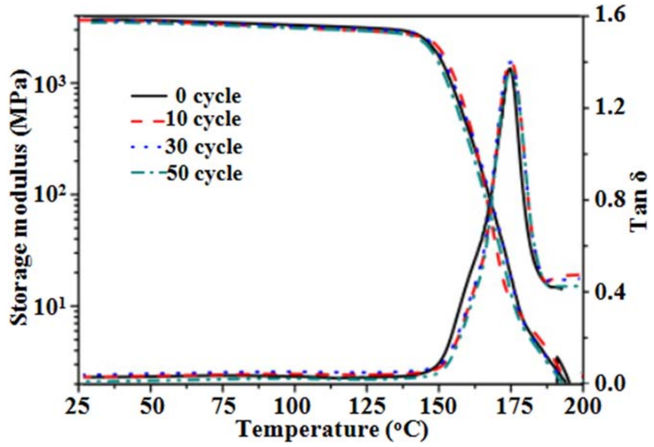

Figure 4. DMA curves of the SMCTPI before and after temperature cycling [145].

earth's shadow [132]. According to the NASA Langley Research Center report, the Space Station in the low earth orbit is expected to be thermally cycled about 175 000 times with an expected life of 30 years [147]. The long-term thermal cycling can result in uneven thermal stress, thermal fatigue, and microcracking of materials, leading to deterioration of physical and mechanical properties.

Leng's group has carried out the thermal cycling experiment for polyimide-based SMP (Tg 170 °C) marked as SMCTPI. The vacuum level, temperature range, cycling times are 5.4×10^{-4} Pa, -170 °C $\sim +170$ °C, 0 cycle, 10 cycles, 30 cycles and 50 cycles respectively [145]. The Tg (the temperature corresponding to the peak of the loss factor **tan** δ) of SMCPI basically stabilizes at 170 °C after 50 cycles (figure 4) [145]. Because the SMCPI has been cured at 210 °C for 2 h in the final step of the curing process [145]. The 210 °C is 40 °C higher than SMCPI's Tg, thus the post-cure effect is not significant during thermal cycling. Fourier transform infrared (FTIR) spectra experiments indicate that the functional groups do not change after thermal cycling (figure 5). Shape memory behavior experiments show the shape fixity and recovery ratio are not significantly altered, confirming the thermal cycling has no significant influence on shape memory property of the SMCTPI [145]. However, material properties with more thermal cycles cannot be estimated based on existing results.

3.3. Ultraviolet radiation

In the space environment, the UV radiation with a wavelength of 10–400 nm, although accounting for a small proportion $\sim$8.7% (118 W m^{-2}) of the solar electromagnetic radiation (1353 W m^{-2}), has a high photon energy, which can cause photolysis and ionization of molecules, cleavage of chemical bonds, resulting in microcracks, cracks, embrittlement and aging. It widely deteriorates the mechanical and optical properties of solar cells, thermal control coatings, composite adhesives, etc [148, 149].

Leng's group has conducted UV radiation experiments of SMP-CRIV and SMCTPI. The irradiation dose for SMP-CRIV and SMCTPI is up to 3000 equivalent solar hours (ESH,

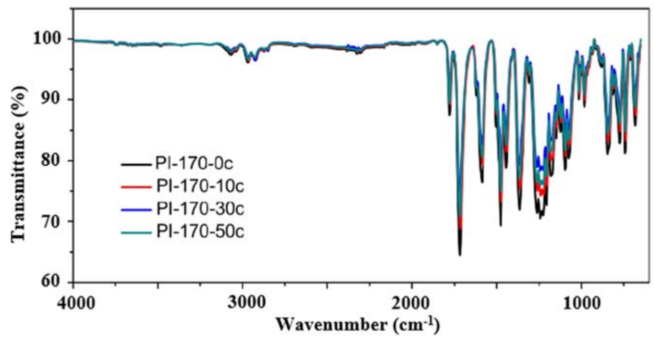

Figure 5. FTIR spectra of SMCTPI before and after temperature cycling [145].

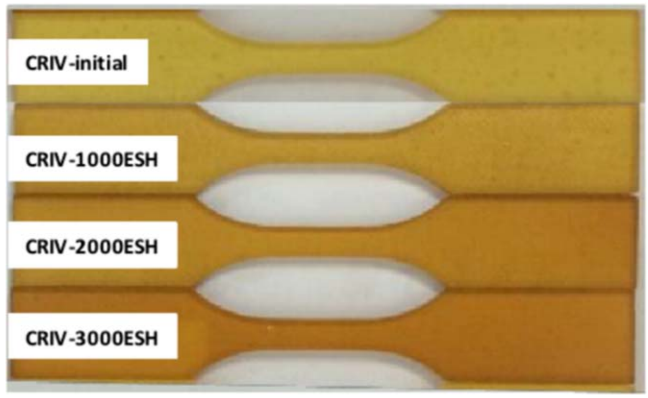

Figure 6. Images of SMP-CRIV samples before and after UV radiation [142].

1ESH $= 1353$ W m^{-2} $\times$ 8.7% $\times$ 3600 s $= 4.2 \times 10^5$ J m^{-2}); the detailed conditions are: wavelength 200–400 nm, 5 times the solar constant, irradiation times of 200, 400, and 600 h, corresponding to 1000 ESH, 2000 ESH and 3000 ESH [142, 145].

The above two types of SMPs have color and transmittance change after high-energy UV radiation since the UV radiation triggers photochemical reactions of materials. The surface color darkens and the transparency lowers in the visible region with the increase of irradiation time, as shown in figure 6. The Tg of SMCTPI is basically unchanged; while the Tg of SMP-CRIV drops by 7 °C after 3000 ESH [142, 145]. The Tg changes for SMPs exposed to UV radiation are complex because the UV could induce either crosslinking reaction or cracking reaction depending on the irradiation dose. Even though the high energy of the UV photons can cause the surface temperature of the material increases after irradiation. The temperature is not high enough for SMP-CRIV's post-curing, so the mechanical properties of SMP-CRIV do not change significantly after irradiation. While the tensile strength and elongation of SMCTPI decrease by 40.5% and 41.79% after 600 h of irradiation, mainly due to the SMCTPI thin thickness, 0.18 mm, which is much thinner than the SMP-CRIV's 2 mm. The effect of UV radiation on material gradually deepens from the surface to inner. For thin SMCTPI, the proportion of the irradiated part is much larger than that of SMP-CRIV, resulting in significant

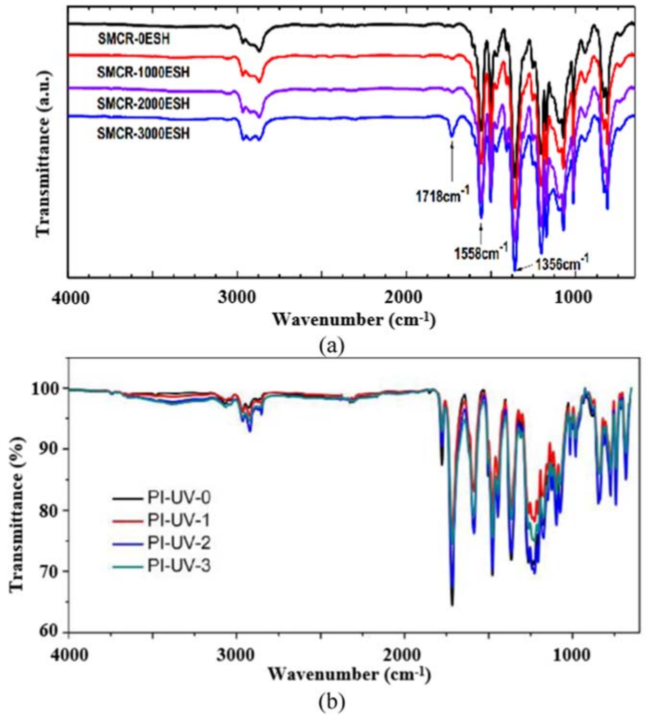

Figure 7. FTIR spectra of materials before and after UV radiation, (a) SMP-CRIV [142], (b) SMCTPI [145].

deterioration of mechanical properties [142, 145]. FTIR experiments and shape memory behavior experiments indicate the UV radiation does not change the chemical bond type of the above SMPs, and their shape memory properties remain stable (figure 7) [142, 145].

3.4. Atomic oxygen

The AO is a kind of free oxygen atoms which is generated by solar UV radiation dissociating oxygen molecules. At low earth orbit (altitude of 300–500 km), the neutral atmosphere consists of 80% AO and 20% nitrogen molecules. When a satellite is operating at 7.8 km s^{-1} in the low earth orbit, the impact energy of atomic oxygen can reach 4.5–5 eV [145]. The high-energy impact can easily break polymer bonds and induce a series of physical or chemical reactions with low activation energy, resulting in surface resin erosion, fiber exposure, mechanical properties degradation, and even the formation of condensable gases which might contaminate the optical instruments on satellites [150, 151].

Leng's group has conducted AO radiation experiments of epoxy-based SMP (Tg 100 °C) marked as SMPEP, and SMCTPI. The experimental condition for SMPEP is lower than that of SMCTPI. The SMPEP is irradiated for 33, 66, and 100 h with AO translational energy of ~5 eV and flux of $>2 \times 10^{15}$ AO cm^{-2} s^{-1} [143]. While the flux is increased to 5×10^{15} AO cm^{-2} s^{-1} for SMCTPI, and the irradiation doses are increased to 3×10^{21} O cm^{-2}, 6×10^{21} O cm^{-2}, and 10×10^{21} O cm^{-2} respectively [145].

As the dose of AO radiation increases, the surface roughness of the material increases. Scanning electron microscope photographs in figure 8 show the morphological

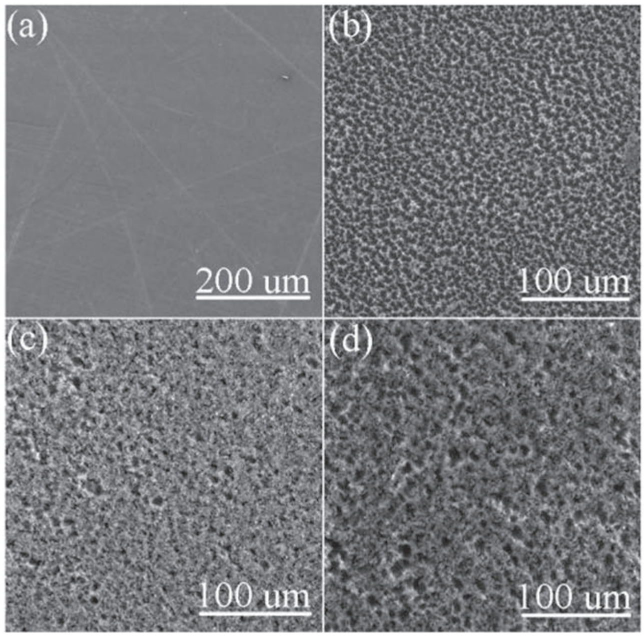

Figure 8. Surface morphologies of SMCTPI samples exposed to different AO radiation doses, (a) 0, (b) 3×10^{21} O cm^{-2}, (c) 6×10^{21} O cm^{-2}, (d) 10×10^{21} O cm^{-2} [145].

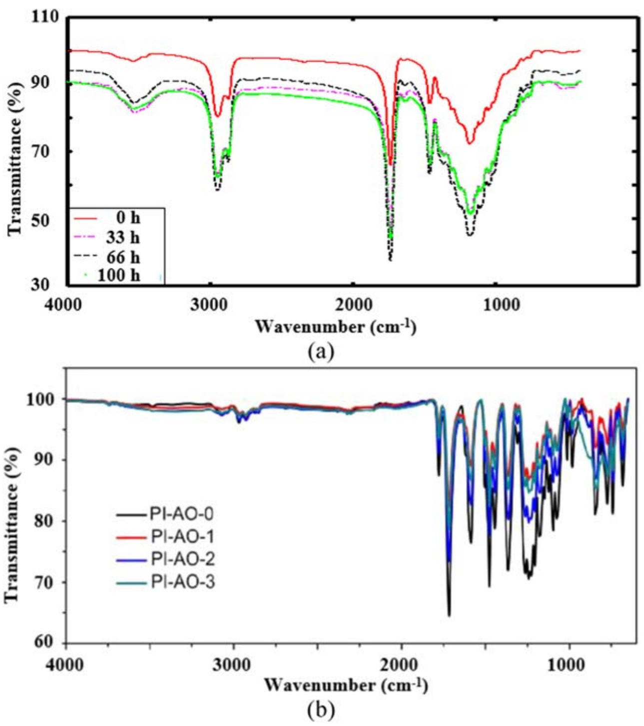

Figure 9. FTIR spectra of materials before and after AO irradiation, (a) SMPEP [143], (b) SMCTPI [145].

transformation of SMCTPI [145]. Because the high-energy impact of AO destroys chemical bonds of material, causing complex oxidation or crosslinking reactions, and generating active particles, such as free radicals, ions, molecules, etc. These products could deposit on nearby surfaces, further causing contamination and altering the surface morphology of materials. The results of FTIR experiments are shown in

Table 3. A list of SMP/SMPC spaceflight experiments.

Time	Experimental type	Experimental object	Experimental content	Material source	Environment	Result
2006	Structure-level	Tembo® EMC hinge	Deploy the experimental solar array	CTD	Low earth orbit: TacSat-2	Success [39, 152]
2007	Structure-level	Tembo® EMC hinge	Measure the recovery force and accuracy of the deployment	CTD	Inside a container onboard the ISS	Success [39, 153]
2007	Structure-level	Deployable gravity gradient boom	Deployment and stabilization of the satellite	CTD	Low earth orbit: FalconSat − 3	The boom was deployed and mostly stabilized the satellite in the z-axis [65, 154, 155]
2011	Material-level	SMP foams under compression, bending and torsion deformation modes	Development in microgravity conditions	3 M Scotchkote™206 N	Inside the BIOKON container onboard the ISS	Recovery ratios for: compression 10%, bending 72%, torsion 71% [70]
2012	Material-level	SMP samples	Development by solar radiation and electrified heating, and long-term observation	SMP Technologies Inc	Exposed outside the ISS	Deployment by solar radiation successfully, but recovery imperfectly by the electrified heating [156]
2013	Material-level	SMP foam, actuator based on SMP foam, SMPC sheet	Development in microgravity conditions	3 M Scotchkote™ 206 N	Inside the BIOKON container onboard the Soyuz spacecraft	Recovery ratios for: compression 88%, actuator 76%, SMPC sheet 90% [71]
2016	Structure-level	A prototype of sunlight-stimulated solar array substrate based on SMPC	Development by sunlight stimulation, and long-term anti-irradiation observation	Jinsong Leng's group	Geostationary orbit: on the deck of an experimental satellite	Success [157]

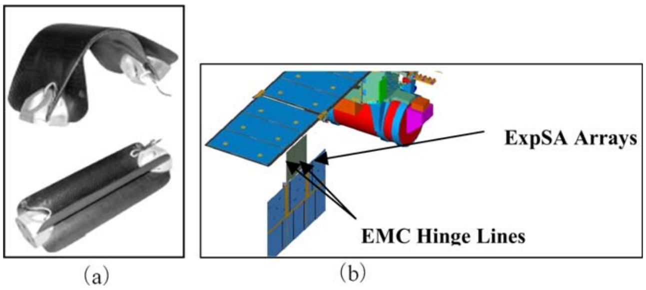

Figure 10. Tembo® EMC Hinge, (a) the images of EMC Hinge in packaged and deployed configurations, (b) TacSat-2 experiment [65].

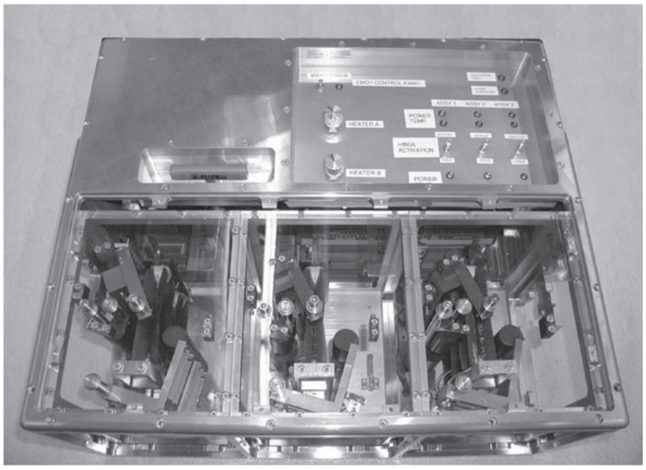

Figure 11. EMC hinge flight unit in International Space Station (ISS) environment [65].

figure 9. After 100 h irradiation, the Tg of SMPEP slightly increases by 3 °C; on the contrary, the Tgs of SMCTPI decreases by ~1.6 °C when the irradiation dose reaches 10×10^{21} O cm^{-2} [143, 145]. The mechanical properties of SMPEP decrease, while almost stable for SMCTPI under different irradiation fluxes. The reason for mechanical properties decrease of SMPEP might be the oxidation reaction between the internal ester bond and the unreacted hydroxyl group on the epoxy resin chain, causing the macromolecular chains which contain C, H, O, N, S to be broken, resulting in microcracks generation and propagation [143, 145]. The microcracks is the main reason for the large decrease of elongation of SMPEP. As we have introduced above, the erosion or degradation of radiation is from the surface to the interior. Since the effect of AO radiation on the internal material is minor, the shape memory property of material would remain the same as those unirradiated ones [143, 145]. The above two SMPs should not be directly exposed to space, they need to be protected when they are used in low earth orbit spacecraft.

So far, the open literature show that CTD Tembo® series have obtained space use licenses, and its products have been conducting spaceflight experiments around 2006 (experimental details will be introduced in section 4). But only the outgassing experiment in vacuum environment has been described in detail; others, such as thermal cycling, UV, etc are just presented with short evaluation words 'good, bad, etc' as results. In recent years, Leng's group has conducted a series of ground-stimulated space environment radiation experiments on epoxy based SMP, polyimide based SMP, and cyanate based SMP. The results show that the above three SMPs have relatively good resistances to space radiations. However, the irradiation dose should not be ignored when evaluating the effect of space radiation on materials, because the effect of any radiation is an accumulation process.

4. SMP/SMPC spaceflight experiments progress

There are a variety of applications of SMP/SMPC on space structures, such as trusses, radiators, and solar arrays, etc. Some of these structures have done spaceflight experiments [39, 65, 70, 71, 152–156]. A brief introduction of them has been listed in table 3. The hinges, deployable gravity gradient boom and the prototype of sunlight stimulated solar array substrate are in structure-level, while the other in material-level.

In the effort to explore the application of Tembo® EMC, CTD has developed a variety of deployment mechanisms and structures, such as hinge, boom, solar array and antennae, most of them have a complete process of design, fabrication, and ground experiments [5, 39, 51, 64, 65, 83]. In the 2000s, Tembo® EMC structures were offered opportunities for spaceflight experiment. Tembo® EMC hinge, two semi-cylindrical carbon fabric reinforced EMC laminates connected by two end fittings, was arranged two spaceflight experiments to evaluate the EMC technology (figure 10). According to the news in NASA website, the first protoflight-level experiment of EMC hinge was its deployment of a experimental solar panel on the satellite TacSat-2 which was launch on 16 December, 2006 [65]. The EMC hinge was approximately 10 cm in length, 2.5 cm in width and height. It was covered by aluminized polyimide thermal shroud, which was used to reduce radiative thermal transfer losses to space while heating the hinge [152].

Another EMC hinge spaceflight experiment was the validation operation of six hinges in International Space Station (ISS) during Expedition 15, from 7 April, 2007 to 21 October, 2007 [153]. This was planned to be the first EMC hinge spaceflight, however, it was carried out after the previous mentioned EMC hinge on TacSat-2 [39, 65]. The test articles were the same size as the hinges on TacSat-2. They were equipped with end fixture, remote actuation and metrology device to evaluate the deployment accuracy, force and torque of the hinge (figure 11). The crew member repeatedly folded the EMC hinges to 90°, the stowed configuration, by using the control panels on the chassis. A full cycle, including power on, hinge deployment and hinge rest, was less than 90 min. The force-torque history and deployment accuracy were automatically recorded but unpublished yet. It was announced that the EMC hinges experiment successfully completed onboard the ISS, confirming the Tembo® EMC hinge, as well as other deployable structures based on

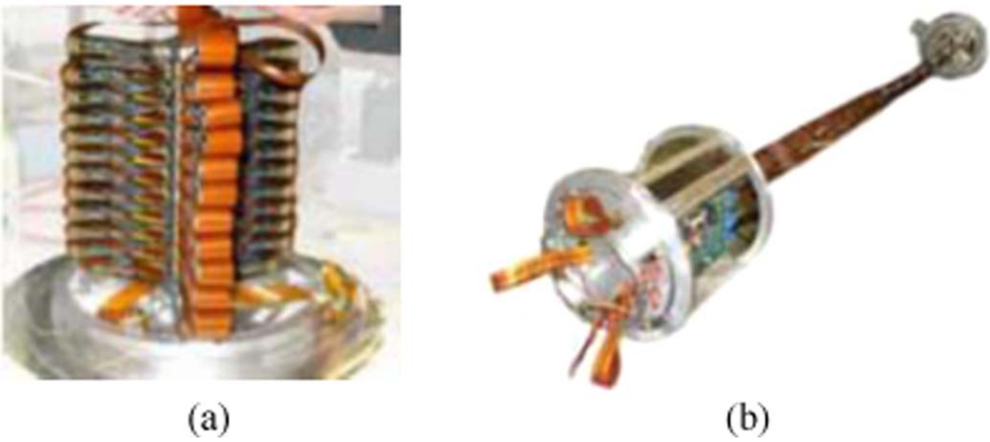

Figure 12. The proposed FalconSat-3 deployable gravity gradient boom, (a) the packaged configuration, (b) the deployed configuration [65].

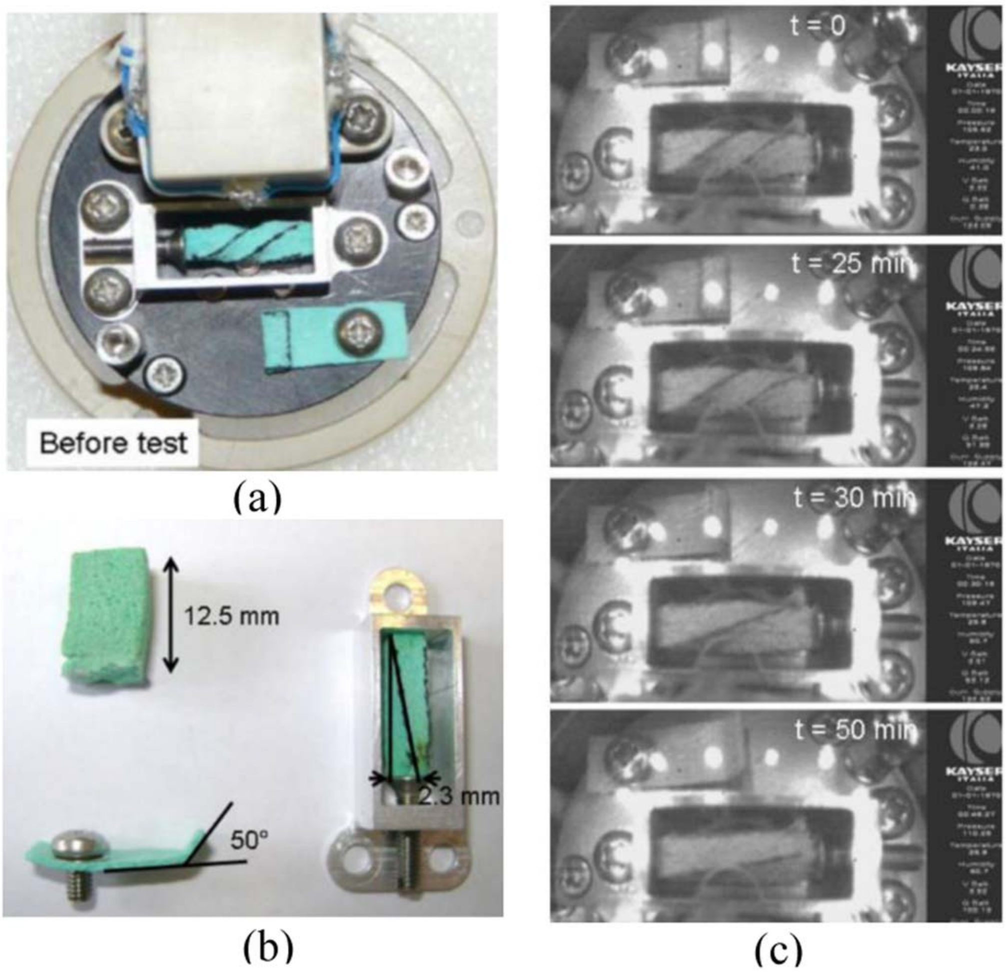

Figure 13. The I-FOAM experiment, (a) initial shape of samples, (b) final shape of samples, (c) progress of recovery in the ISS [70].

Tembo® EMC material could be used for space applications [153].

The deployable gravity gradient boom was one of important scientific loads for FalconSAT-3, a student-built microsatellite, which was launched on 9 March, 2007 [154]. The boom belongs to Tembo® EMC deployable boom structure of CTD, aiming to verify the material-level deployment technique. It was mounted with a tip payload and used for the passive gravity gradient stabilization of the satellite. It was designed with central sleeves and EMC longerons (figure 12). The longerons were EMC laminates, which were folded in a serpentine fashion for launch. Once on orbit, the laminates were heated for deployment thus providing driving force to deploy the boom. The expanded boom was 3.3 m long, and its total mass was 10.6 kg (tip payload mass 8 kg). On 28 November, 2007, the boom was deployed

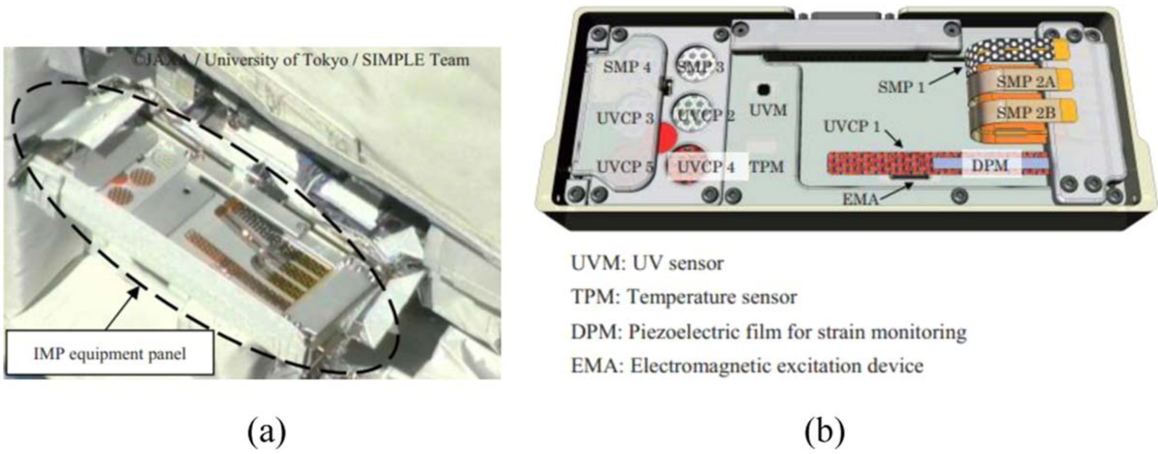

Figure 14. Inflatable Material Panel (IMP), (a) overall view of IMP during spaceflight, (b) specimen layout of IMP [156].

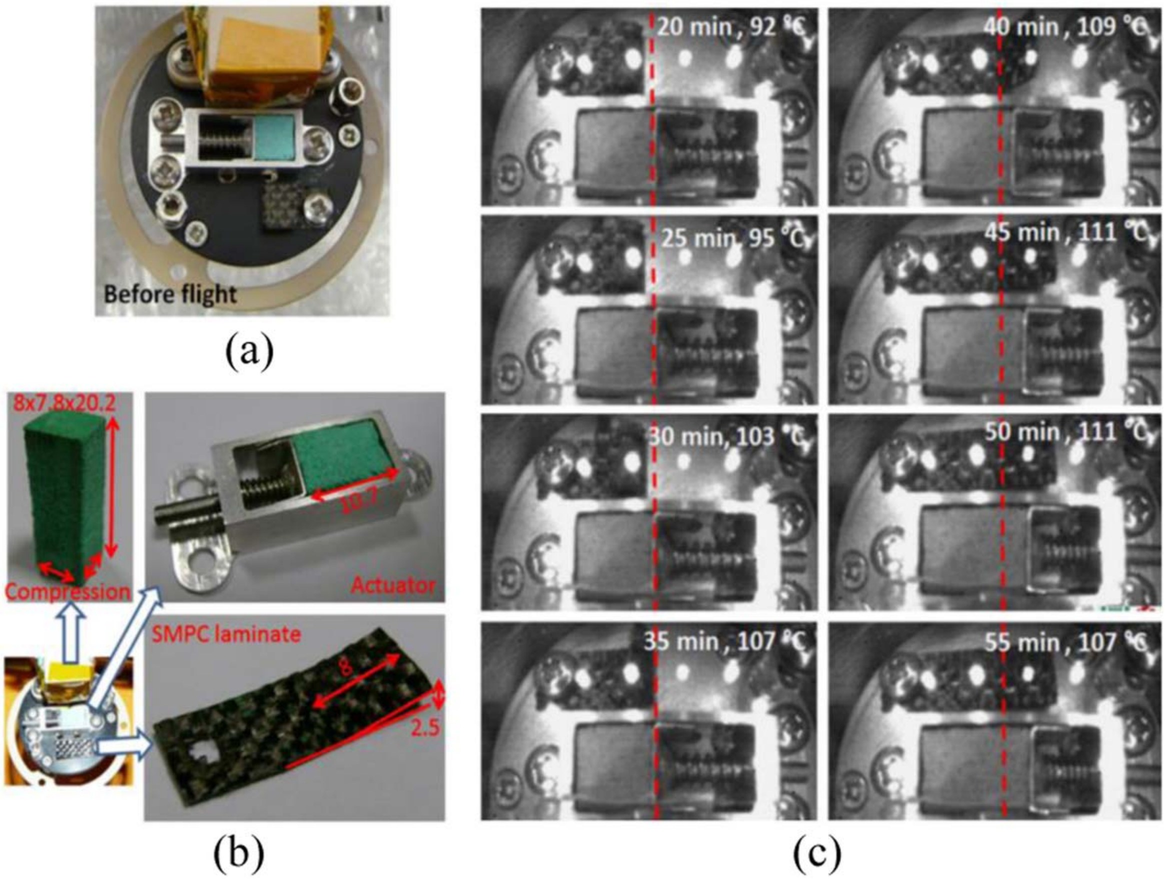

Figure 15. The Ribes_Foam2 experiment, (a) the samples and experimental unit before flight, (b) size of samples after flight, (c) images of recovery during heating on-board [71].

and mostly stabilized the satellite in the z-axis [155]. The gravity gradient boom for FalconSat-3 is a successful application of SMPC in the low earth orbit, and provides a cutting-edge and efficient mechanism for deployable trusses.

In the 2010s, Italy, Japan and China have joined the SMP/SMPC spaceflight experiments [70, 71, 156, 157]. The I-FOAM experiment in microgravity conditions was carried out on 22 May, 2011, during the Shuttlem Mission STS-134 (ISS assembly flight ULF6) [70]. There were three foam samples under different loading conditions: compression, bending and torsion. They were placed in the BIOKON container which could be taken back to earth for further analyses after the spaceflight (figure 13). All samples did not achieve the full recovery, recovery ratios of 10% for compression, 72% for bending and 71% for torsion deformation [70]. After comparing with ground laboratory experiments, scientists and engineers drew the conclusion that the microgravity had no influence on shape memory property of the

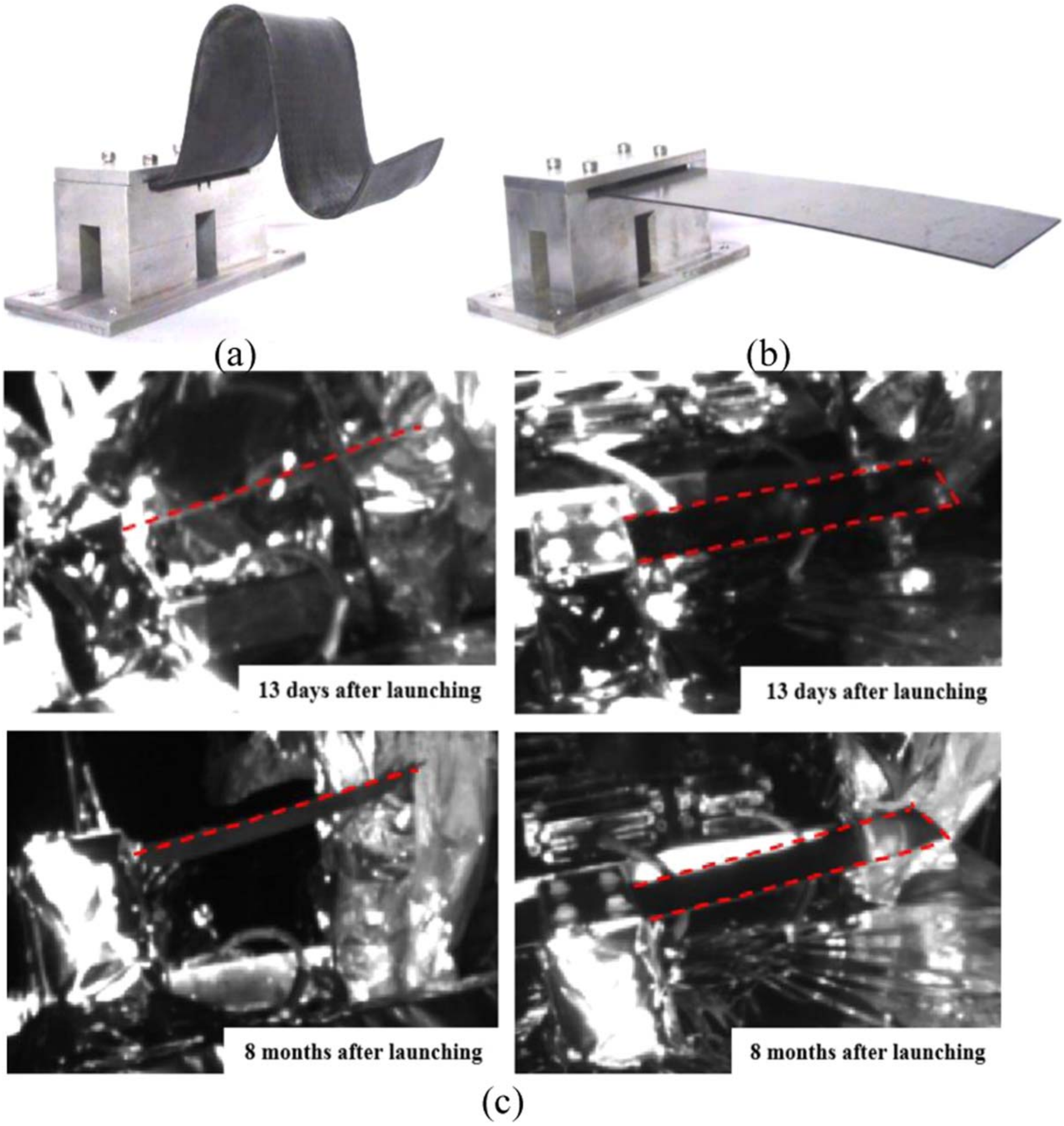

Figure 16. Mission SMS-I, (a) the packaged configuration, (b) the deployed configuration, (c) orbital images 13 d and 8 months after launching [157].

foams but did affect the behavior of heating devices, thus the bad heating condition affected the shape recovery. In the following Italian SMP spaceflight experiment, Ribes_Foam2 (2013), the heating problem was solved [70].

According to the timeline, we need to introduce the Inflatable Material Panel (IMP) experiment of Japan before the Ribes_Foam2. The IMP was an experimental sub-mission equipment of the Space Inflatable Membranes Pioneering Long-term Experiments, which was installed to the exposed facility on Japan Experiment Module in ISS on 9 August, 2012 [156]. The SMP samples had two kinds of surface to space environment, one was naked and deployed by solar radiation, the other was covered by thermal control film and deployed by electrified heating (figure 14). The configuration of sample stimulated by electrified heating was slightly different from the original, which might be caused by the effects of excessive heating and stress relaxation [156]. It was also planned to evaluate the resistance of these samples to long-term radiation, but we failed to find any update.

On 20 April, 2013, Ribes_Foam2, another SMP spaceflight experiment by Italy, was performed during Mission BION-M1 of the Soyuz spacecraft [71]. The equipment was the same as that of in the I-FOAM. Only the compression deformation was repeated, the other two were replaced by a small actuator which was actuated by SMP foam, and a SMPC sheet (figure 15). The first goal was to overcome problems which caused the incomplete recovery of foams in the I-FOAM. Others are the data collection of actuation load during recovery of compressed foam, and the recovery behavior testing of carbon fabric reinforced SMPC. Recovery

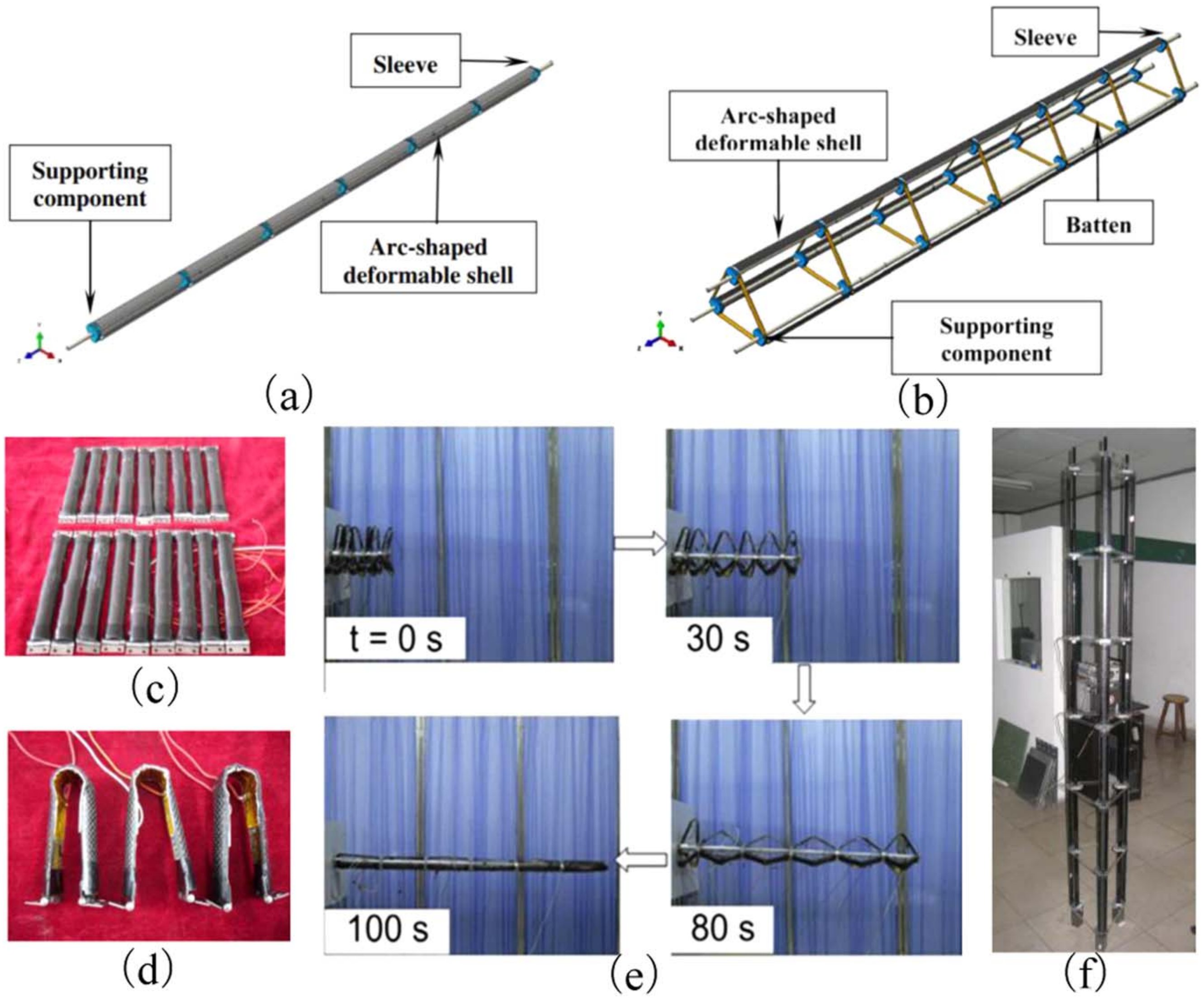

Figure 17. Two kinds of deployable trusses, (a) schematic of the three-longeron beam, (b) schematic of the three-longeron truss, (c) unfolded SMPC laminates, (d) folded SMPC laminates, (e) the deployment process of the three-longeron beam, (f) the modal of the three-longeron truss [50, 165].

ratios of the compressed SMP foam block, the SMP foam in actuator and the SMPC sheet are 88%, 76%, 90% respectively. In Ribes_Foam2 experiment, 100% shape recovery was not achieved, but much better than those in I-FOAM. The main reason is that the heating phase in Ribes_Foam2 (55 min) is longer than the previous one (25 min) [71].

In 2016, a prototype of sunlight-stimulated solar array substrate based on carbon fabric reinforced SMPC, named Mission SMS-I, was carried by an experimental satellite to the geostationary orbit to do the deployment test and long-term anti-irradiation observation [157]. The substrate exhibited the 'Ω' packaged configuration, and could recover to the '—' deployed configuration upon sunlight stimulation (figure 16). The Tg of the epoxy-based SMP matrix was 85.4 °C. The first order of natural frequency for the packaged substrate was 35.17 Hz, while 2.07 Hz for the deployed substrate. Due to the operation limitation, the orbital deployment process has not been recorded, only images of the deployed substrate were obtained. The substrate was found deployed to the '—' configuration with a recovery ratio of ∼100% at the first observation thirteen days after launching. It maintained the straightly flat configuration without visible crack eight months later, indicating the SMPC had a good long-term anti-irradiation capability [157]. The Mission SMS-I is China's pioneering SMPC orbital experiment, and the world's first SMPC geostationary orbit experiment. Its significance is to demonstrate the possibility of the passive deployment mechanism, and the availability of SMPC directly exposed to the geostationary space environment.

Published spaceflight experiments of SMP/SMPC have boosted the research enthusiasm for new shape memory materials and structures. Various structures, including hinge [158], flexible solar array [159], deployable mirror [64], and hinge driven reflector [160, 161], have been developed and conducted ground-based tests, but lack the opportunity for spaceflight experiment.

Figure 18. Deployment process of the self-deployable tube [38].

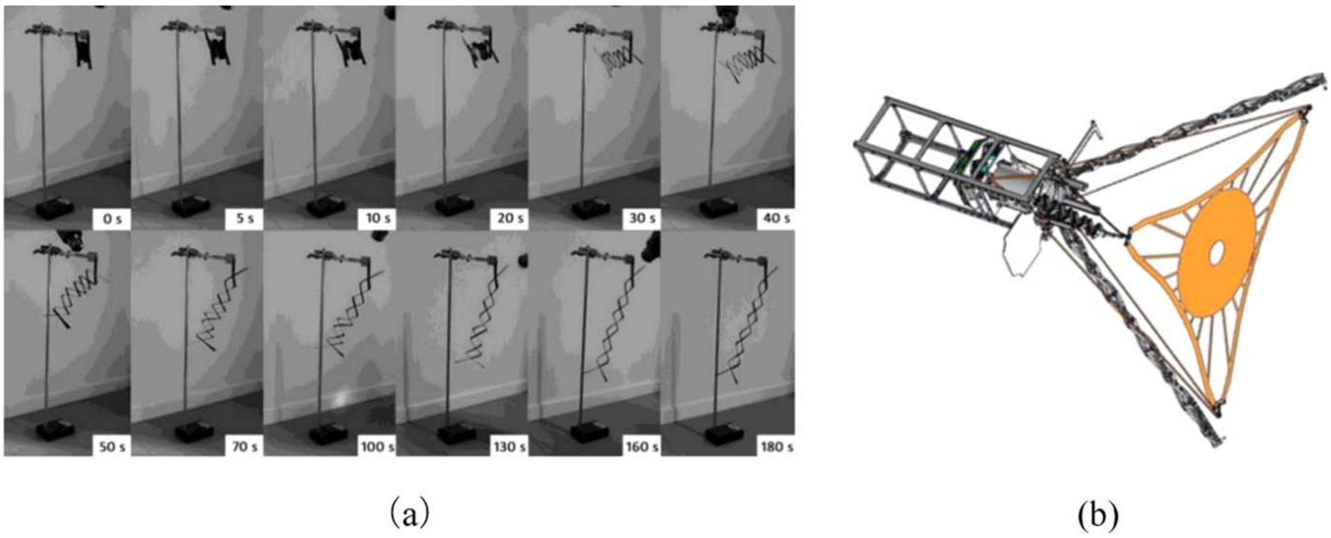

Figure 19. Repeated X-shape mast based on SMPC, (a) deployment process, (b) potential application at deployable membrane telescope for a CubeSat [166, 167].

5. Potential applications of SMP/SMPC in aerospace field

At present, there are still many researchers focus on developing SMPC hinges and booms, most of which are based on the EMC hinge and boom developed by CTD, but have been refined in material preparation, structural optimization and testing method to meet different engineering requirements [50, 158, 162]. Some new applications, such as the wrinkled/slack control component, the release devices, the solar arrays, and the deployable trusses with new configurations, have been developed [28, 163, 164]. They may not have attracted much attention at the moment, but have promising prospects and can provide inspirations for new application development.

Leng's group developed two deployable trusses: the three-longeron beam and the three-longeron truss (figure 17) [50, 165]. The three-longeron beam was similar to the gravity gradient boom of the FalconSAT-3 mentioned above, consisting of an extensible central sleeve rod and 120° distributed SMPC laminates around the sleeve. But its cross-sections of the same-stage sleeve were in the equal sense for reducing the friction [50, 51]. The three-longeron truss had three parallel placed sleeve rods to form an equilateral triangle cross section. SMPC laminates were overlain the outside of each sleeve rod [165]. Both deployable trusses had six stages, with three SMPC laminates at each stage, establishing 'V' shape in the packaged configuration and '—' shape in the deployed configuration. Figure 17(e) shows the deployment process of

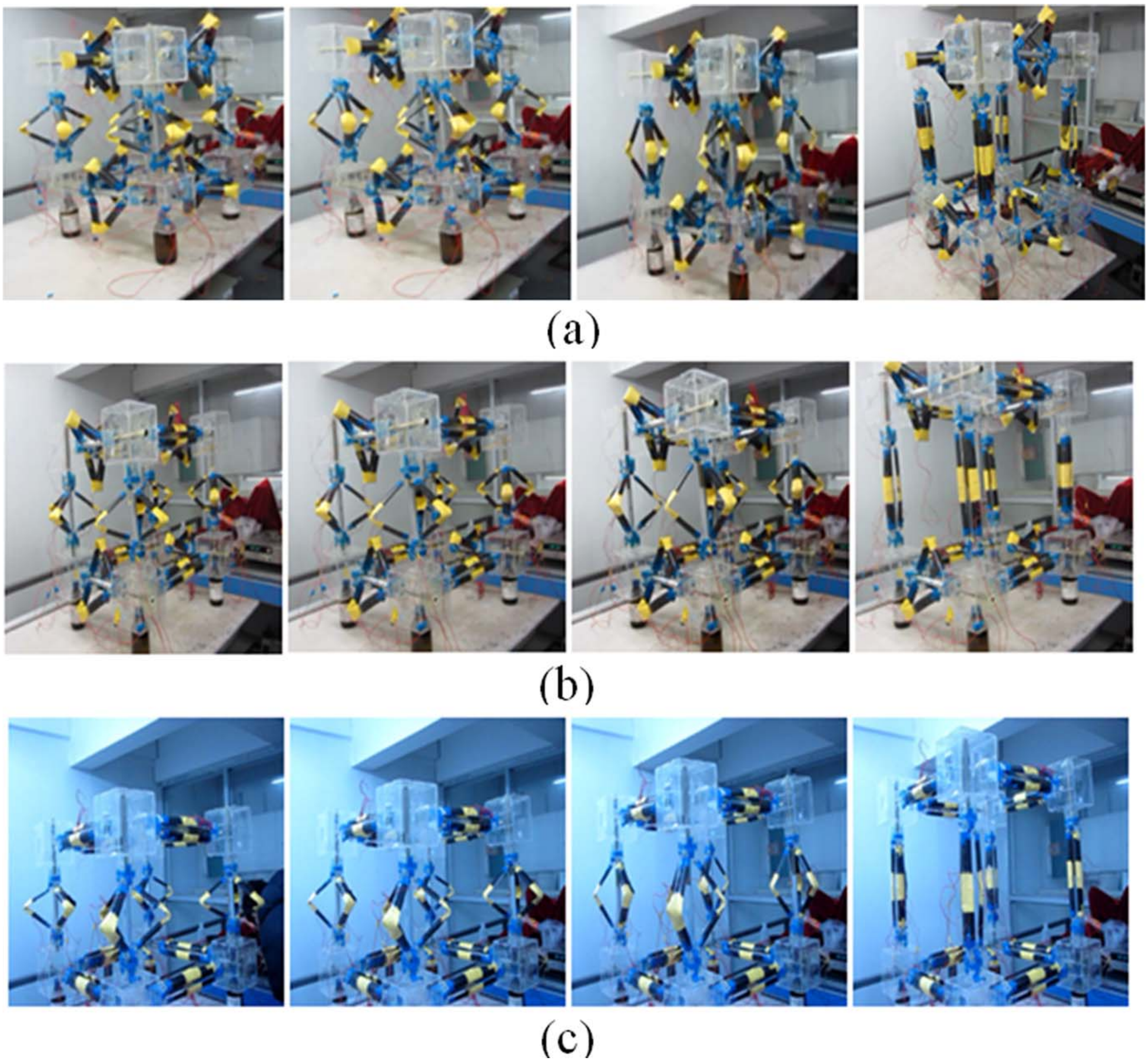

Figure 20. The deployment process of the cubic deployable support structure, in the first direction, (b) in the second direction, (c) in the third direction [82].

the three-longeron beam. The deployment speed was slowly at the beginning, then increased as the temperature reached the Tg of the SMPC, and finally tended to zero; the whole deployment lasted about 100 s [50]. The stiffness of the truss was higher than that of the beam, their first order of natural frequencies were 980.13 and 935.84 Hz in sequence [165].

Unlike the EMC hinge mentioned above, Liu *et al* introduced an integrative hinge which was hollowed out along the side of a SMPC tube to form two symmetrical arc-shape laminate with an arc angle of 120°, and developed a self-deployable tube based on the integrative hinge (figure 18) [38]. The self-deployable tube is packaged in a serpentine fashion, and can be deployed in a predetermined path by heating different hinges. The first order of natural frequency was 101.3 Hz. The deployment time for the hinge with 180° folding angle was ~60 s, but could be adjusted by varying the matrix type, composite dimension, and actuation power [38]. The number and length of segment, the bending angle can be optimized to meet different requirements. It has good characteristics of none complex mechanical devices, material-level deployment, lightweight and relatively high stiffness. The integrated design concept is a good way to improve the stiffness of new structures. The fewer the detachable joints, the higher the stiffness of the deployed structure.

Santo *et al* made a repeated X-shape mast based on SMPC. It consists of two SMPC strips which are combined at two intersecting cuts and bent to about 180° in the center portion of the strip between the two consecutive cuts (figure 19(a)). A small mast has been prototyped and completed the deployment test to demonstrate the feasibility of

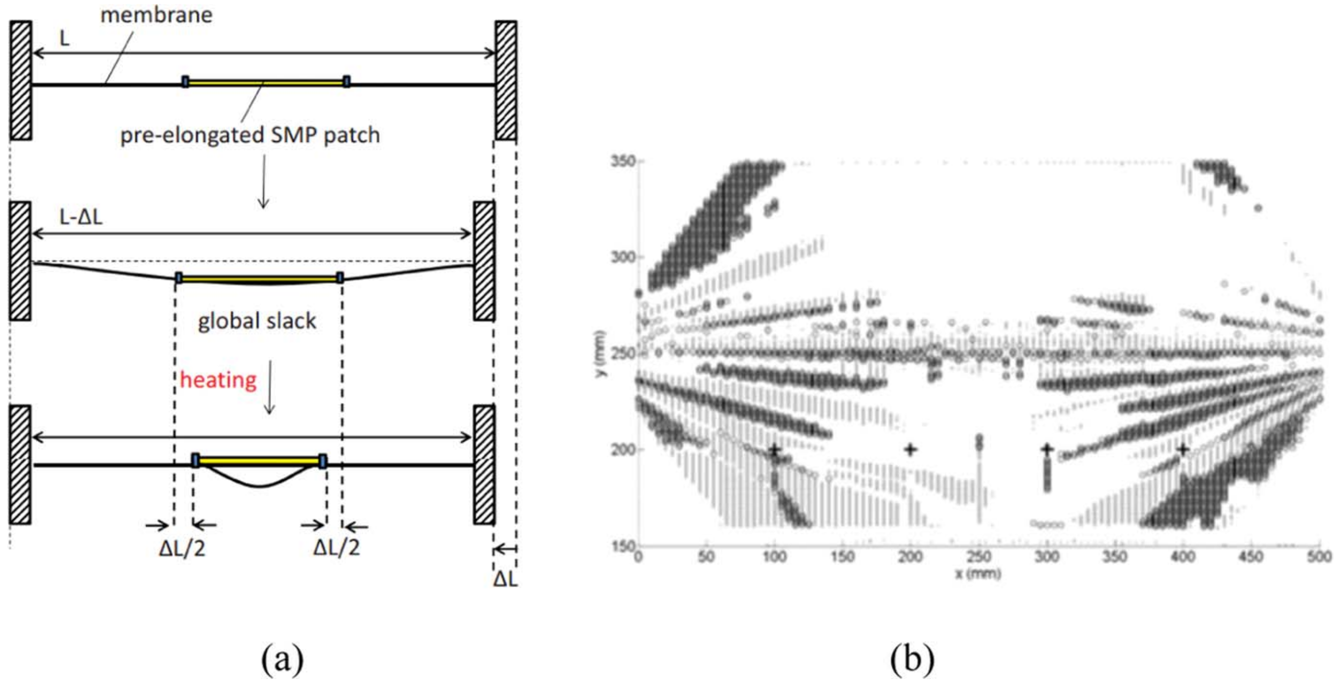

Figure 21. SMP films for wrinkled/slack control, (a) schematic of the shape control concept by attaching a SMP film on the membrane's surface, (b) comparison of the measured out-of-plane displacement before and after the SMP film wrinkle control [163].

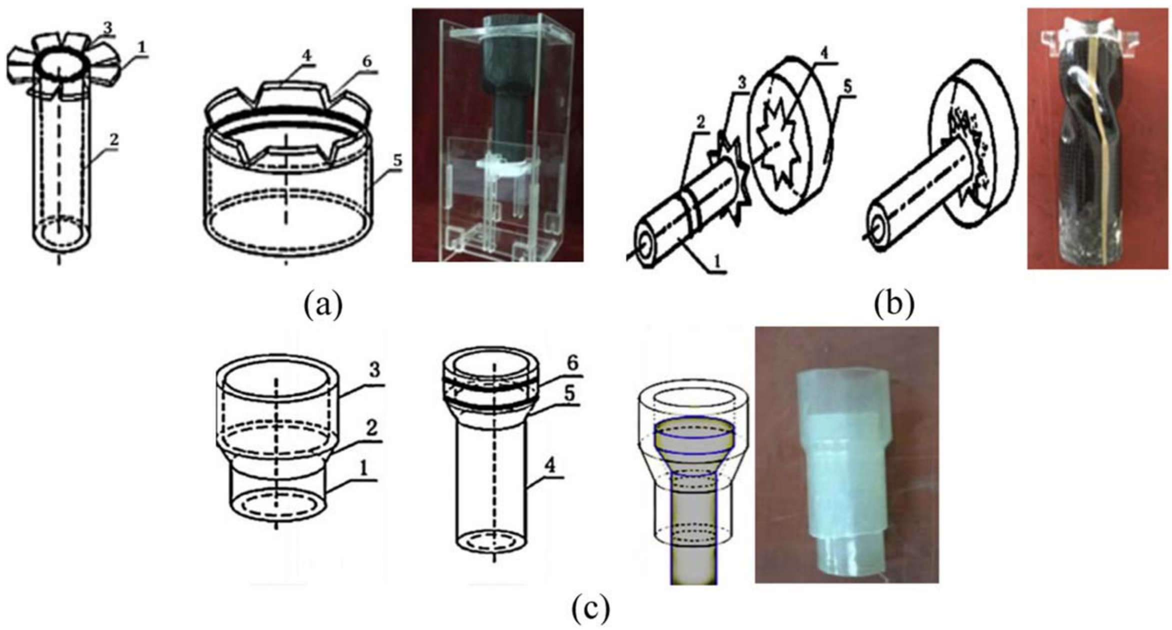

Figure 22. Smart release devices, (a) the 'Lotus' device, (b) the 'Eight paws' device, (c) the 'Bamboo' device [28].

this structure. It can support membrane structures, such as small antennas, membrane telescopes, etc (figure 19(b)) [166]. Li *et al* developed a cubic deployable support structure consisting of three-longeron SMPC trusses (figure 20). The functional component is the arc-shaped SMPC laminate that provides the recovery force for deployment. The whole structure could be deployed in three perpendicular directions. It could be used as the driving mechanism and support structure for inflatable systems [82]. Santo's X-shape mast and Li's cubic deployable support structure are all based on the basic SMPC laminates. They modified and assembled the basic laminate to new structures for specific application backgrounds. The ingenuity inspires us to deconstruct complex structures into simple components, and eventually assemble them into pre-conceived structures.

We have discussed the deployment method for space deployable structures, but rarely involve other components in the whole structures, such as ultra-thin films in space reflector, occluder, and solar sail, etc. For membrane structures with long-term missions, slight changes in surface can

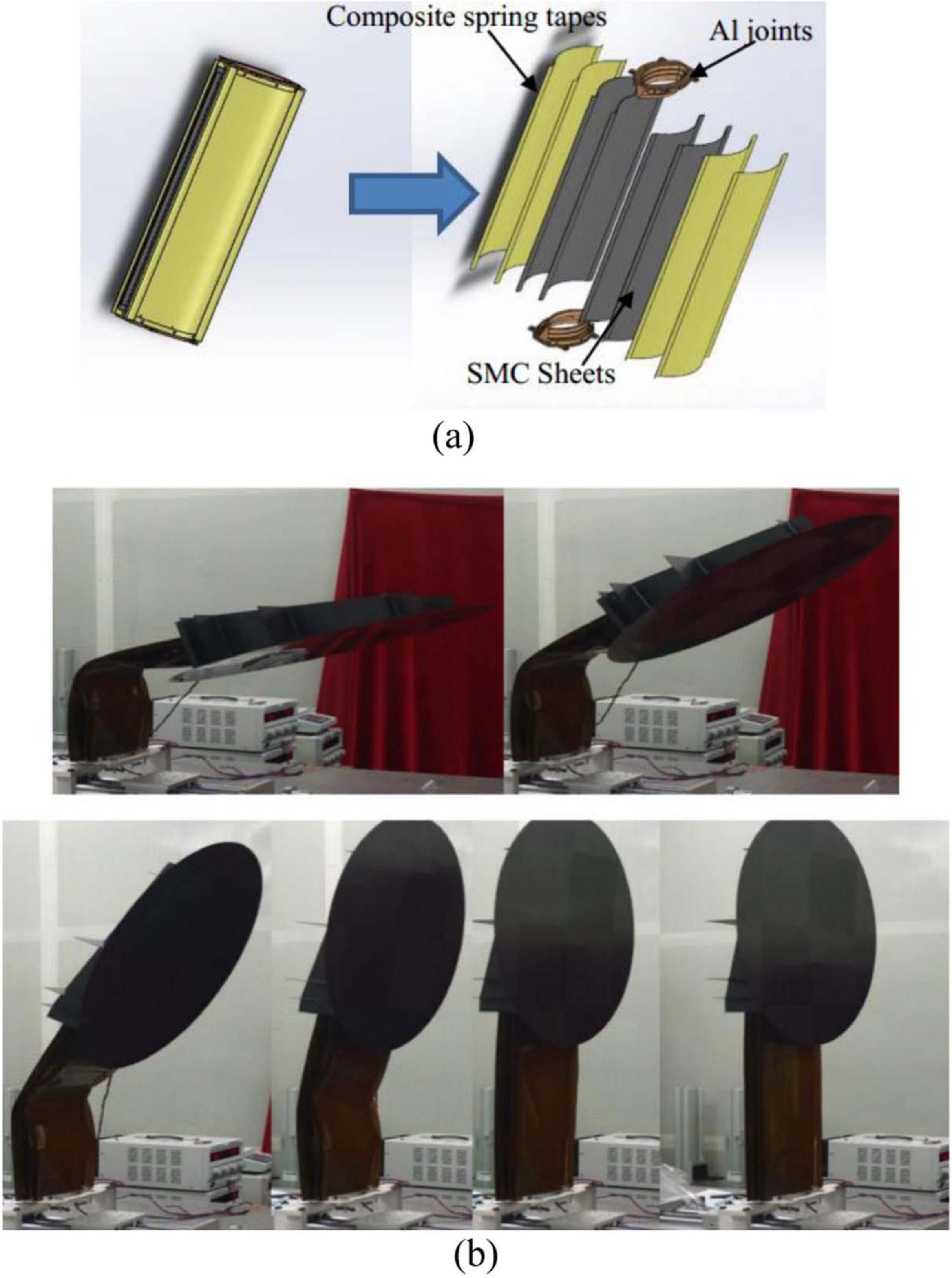

Figure 23. Space deployable mechanism (SDM), (a) configurations of SDM, (b) the deployment process [162].

severely affect their mechanical property and response accuracy. How to overcome or reduce the indispensable creep is a challenging issue. In 2013, Senba *et al* presented a novel patch-type SMP film for wrinkled/slack control of large membrane structures (figure 21) [163]. Each SMP film was pre-elongated before attaching its ends to the membrane. When needed, the SMP film was heated above its Tg. The recovery force was transferred to the membrane through attached ends to change the membrane's out-of-plane displacement distribution to reduce the wrinkled/slack area. Once the SMP film cooled below Tg, its shape can be fixed. Results showed that the effect of the SMP film on the

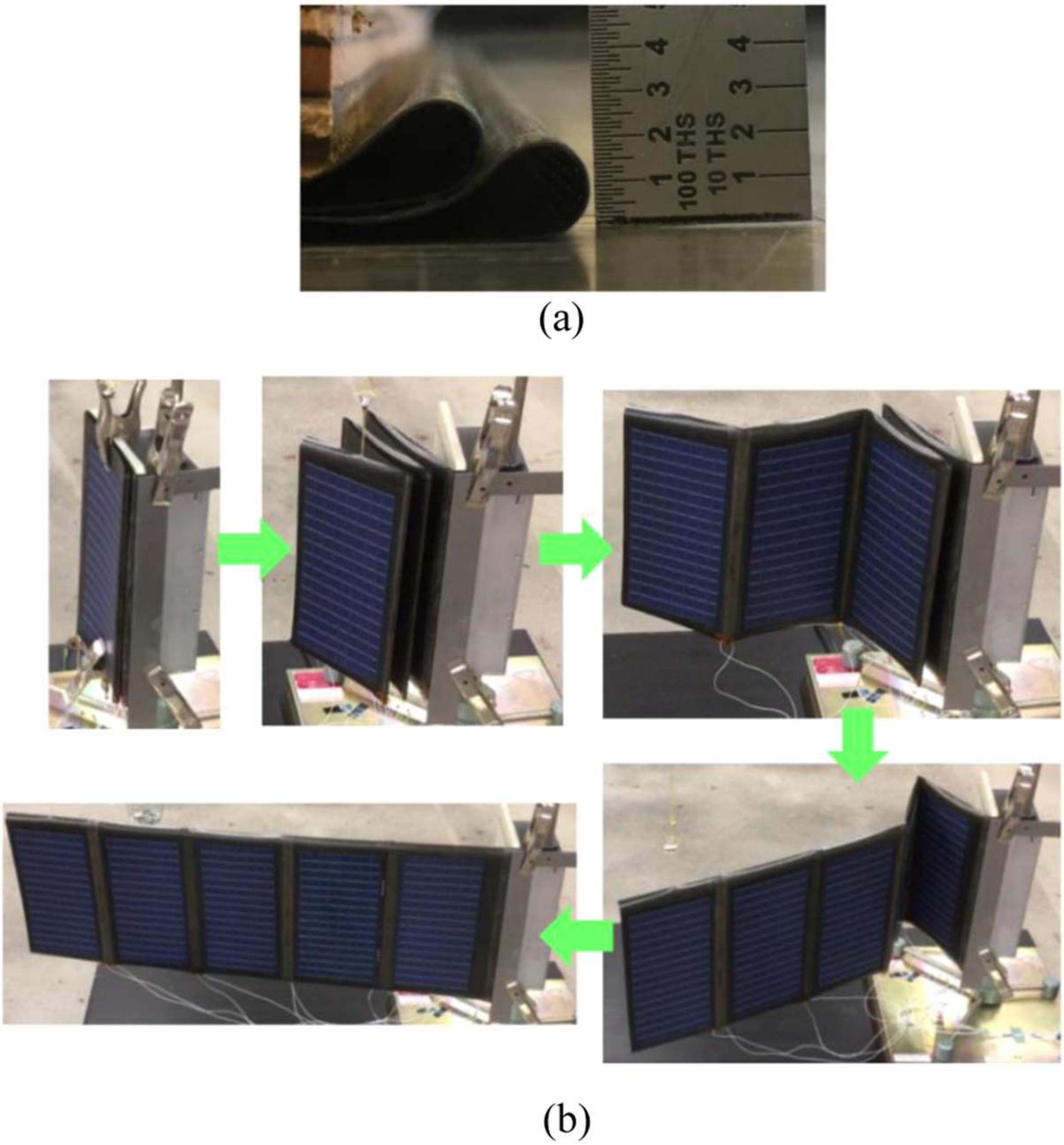

Figure 24. Composite lightweight array using shape-memory polymer (CLASP), (a) nested (P-folded) hinge-line, (b) deployment process of CLASP on a mock 6U CubeSat [164].

wrinkled area was very localized in region close to it, and the out-of-plane displacement on the slake area was drastically reduced [163]. The stress distribution in the membrane should be considered to optimize the position of the SMP film. This application is a good example of the structure that values both shape fixation and recovery capability of the shape memory component, since the SMP film here must maintain the stretched length before the recovery operation.

Another application values the shape fixation of SMP/SMPC is the release device. Wei *et al* presented three smart release devices based on carbon fiber reinforced styrene-based SMPC (figure 22) [28]. Their names are ‘Lotus’, ‘Eight paws’ and ‘Bamboo’ device respectively, corresponding to the bending, twisting and shrinking deformation modes at the mating portion. The locking loads of the ‘Lotus’ and ‘Bamboo’ devices were obtained by tensile tests, where the maximum load of ‘Bamboo’ was 430 N, which was higher than the 284 N of ‘Lotus’. The ‘Eight paws’ failed to get the maximum load due to the debonding of paws and the SMPC cylinder [28]. They can be completely released in less than 30 s. Unlike conventional explosive bolt release devices, new devices have no pyrotechnics, which reduces the cost and shock upon release. However, the locking load is much lower, which limits the application. Devices with larger locking load are under development. The above-mentioned Senba’s SMP film and Wei’s smart release devices prove that SMP/SMPC can be applied not only to space deployable structures, but also to many other structures involving various deformations.

In 2017, Chen *et al* developed a new space deployable mechanism (SDM) which was essentially a larger hinge but with different components and configuration compared to the EMC hinge. Besides the internal SMPC sheets, composite spring tapes (CSTs) for improving the global stiffness and deployment force, and aluminum alloy end joints for securing the SMPCs and CSTs together were integrated into the SDM (figure 23(a)) [162]. An experimental SDM prototype with a radius of $\sim$0.19 m, a length of $\sim$0.50 m and a weight of 2.142 kg was fabricated, and repetition experiments of the structural stiffness and shape recovery rate were conducted. Results indicated that the bending stiffness of the SDM along X axis is $\sim$5000 N m^2 [162]. The SDM could effectively recover at least 10 times with shape recovery rate over 99.994% [162]. It successful deployed an antenna reflector as shown in figure 23(b). The SDM inspires us to apply other materials, such as the CST here, to conventional SMPC to improve the basic mechanical properties.

In 2018, Rakow *et al* introduced a new Composite Lightweight Array using shape-memory polymer (CLASP) for small spacecrafts that require larger area and higher packaging efficiency of solar arrays [164]. CLASP was a Z-folded solar array that incorporated Tembo® EMC hinges spanning the whole width of the edge to connect adjacent carbon fiber composite substrates. Once deployed, the CLASP had a continuous surface. This design not only increases the stiffness and strength of the solar array, but also increases the stowed volumetric efficiency since the EMC hinge-lines are packaged in a P-folding shape and stacked tightly (figure 24(a)). The dimension of the deployed CLASP was 1.0 m long and 0.36 m wide. A CLASP prototype has been packaged and deployed multiple times on a side wall of a mock 6U CubeSat. EMC hinge-lines were developed from the farthest to the root of the CubeSat, as shown in figure 24(b) [164]. More ground-based qualification tests are planned, including thermal vacuum deployment and vibrations.

SMP/SMPC could be combined with origami/kirigami technology, considering the crease pattern and behavior of origami/kirigami are suitable for designing large deployable structures. Recently, Chen *et al* published a new solar array based on origami and SMP actuators [168]. It is mainly composed of a Hoberman ring and an elastic origami substrate. The Hoberman ring, which is a series of scissor mechanisms in a circle, forms the structural support system and the actuation mechanism. The elastic origami substrate embedded in the round of the Hoberman serves as the secondary actuation and provides the deployable surface to carry solar cells. The hub of Hoberman ring and the base layer of the origami substrate were made of SMP. Both of them were fabricated by 3D printing. They were printed in expanded configurations, assembled together by hooks, then packaged into a cylinder, and finally deployed in hot water with an expansion ratio of 1000% and development time of 40 s. The origami folding method provides the possibility of achieving a higher expansion ratio than the conventional accordion folding. However, most crease patterns there are irregular, preventing the effective use of the area, thus related accessories for crease pattern optimization need to be developed.

6. Conclusion

SMP/SMPC has important application value in the aerospace field, but to achieve commercial applications, they need to integrate a variety of excellent functions, such as good space radiation resistance, stable shape memory performance, suitable mechanical properties, simple and effective stimulus methods, etc. It is essential to know that the shape memory behavior is a general phenomenon of polymeric materials, just differ in recovery time. The SMP/SMPC stands out mainly because of its remarkable shape fixation and shape recovery capability. All aerospace-grade materials are required to do the space radiation verification. This review lists four radiations, including high vacuum, thermal cycling, UV, and AO, and shows the epoxy, cyanate and polyimide-based SMPs have good performance under certain radiation doses. Various space structures based on SMP/SMPC have been developed. The spaceflight experiments of SMP/SMPC in open literature, varying from the material-level (the foams and composite synthesized by Santo *et al* [70, 71], and the SMP samples with different surface developed by Aoki *et al* [156]) to the structure-level (the EMC hinges and the deployable gravity gradient boom developed by CTD [39, 65, 153], and the sunlight-stimulated solar array substrate prototype developed by Leng's group [158]), demonstrate good shape recovery capabilities of material or structure in actual space environment. However, most of the SMP/SMPC based structures do not have the opportunities to spaceflight experiments but the ground verification tests. These structures include the deployable trusses [38, 50, 165, 166], the cubic deployable support structure [82], the mesh-surface antenna [51], the hinge [162], and the deployable solar array [164, 168], etc, which can deploy successfully by using bending deformation and show great potential for future application. Besides the commonly used bending deformation and the shape memory property of the material, the potential structures adopt tensile (the wrinkled/slack control component [163]) torsional (the 'Eight paws' release device [28]) deformation modes, and utilize the shape fixation capability of the material to develop new structures.

7. Future outlook

The SMP/SMPC can be conceived as various components as long as they are deformable, portable. The research of SMP and SMPC have experienced rapid and even explosive growth. The current developments of SMP/SMPC in aerospace applications have been reviewed above. This section will give an outlook to the future study.

1. The working conditions, reliability and service life of the spacecraft are closely related to the space environment. It is necessary to study the effects of the space irradiation on materials, exploring the degradation or erosion mechanisms, and find out proper protective methods. It should be noticed that the actual space

environment is a combination of various radiations, and the coupling effect of multi-space environmental radiations on materials is temporarily unknown. Providing a new material spaceflight experiment opportunity will be the most direct and effective way to evaluate the material's resistance to space radiations.

2. Larger but relatively lighter deployable structures are always expected, especially for solar array, solar sail, antenna, etc. Origami and kirigami have been introduced to conceive the geometrical design of SMP/SMPC-based structure. With crease pattern design, high deployed-to-packaged ratio can be achieved. SMP/SMPC is mainly used as hinges at creases, the materials-level deployment mechanism reduces the mechanical complexity of the system. The thickness of the material needs to be considered during the pattern design. Mathematical models have been proven useful in facilitating the crease pattern modification to accommodate the material thickness. But practical modification is still needed to fabricate and test physical products.
3. Most of the SMP/SMPC used in aerospace applications is thermal-induced material. Deforming a SMP /SMPC component requires the presence of heat since both packaging and deployment need to be implemented above the material's Tg. Currently, the resistance film stuck or embedded in the material is always used as a controllable electrical stimulation. But the failure of electricity supply would lead to unpredictable anomalies and even affect the entire spaceflight mission. The sunlight-stimulated deployment mechanism could be a remedy of deployment anomaly since the sunlight is stable and procurable. It also saves the power during deployment.
4. It is crucial that those SMP/SMPC based structures can be deployed controllable with high precision and accuracy. The shape recovery speed and ratio are affected by various factors, such as the material itself, the structure form, the environment, especially the stimulation system. Additional sensors could be installed to monitor the deployment level and return data to aid the control of the stimulation system, such as the heating power and heating time for thermal-induced SMP/SMPC.
5. The SMP/SMPC mentioned above only has the 'one-way recovery' capability, that is, it just recovers from the 'deformed shape' to the 'original shape', and it is impossible to achieve the reversible switching between the two states without external force. Therefore, the application based on SMP/SMPC is mostly a one-time deployment structure. Reversible deformation without the need for repeated programming, also known as the 'two-way shape memory effect' for SMP /SMPC has arisen [169–171]. Although they are still in the material development stage, preliminary progress has made people see its feasibility in artificial muscles, soft actuators, grippers and optical gratings, etc [170, 171].

Acknowledgments

This work is supported by the National Natural Science Foundation of China (Grant Nos: 11672086, 11772109 and 11632005) and China Scholarship Council.

ORCID iDs

Yanju Liu https://orcid.org/0000-0001-8269-1594
Jinsong Leng https://orcid.org/0000-0001-7249-9101

References

[1] Behl M and Lendlein A 2007 Shape-memory polymers *Mater. Today* **10** 20–8
[2] Leng J, Lan X, Liu Y and Du S 2011 Shape-memory polymers and their composites: stimulus methods and applications *Prog. Mater Sci.* **56** 1077–135
[3] Liu T, Zhou T, Yao Y, Zhang F, Liu L, Liu Y and Leng J 2017 Stimulus methods of multi-functional shape memory polymer nanocomposites: a review *Composites* A **100** 20–30
[4] Lendlein A, Jiang H, Jünger O and Langer R 2005 Light-induced shape-memory polymers *Nature* **434** 879
[5] Zhang H, Xia H and Zhao Y 2014 Light-controlled complex deformation and motion of shape-memory polymers using a temperature gradient *ACS Macro Lett.* **3** 940–3
[6] Heuchel M, Razzaq M, Kratz K, Behl M and Lendlein A 2015 Modeling the heat transfer in magneto-sensitive shape-memory polymer nanocomposites with dynamically changing surface area to volume ratios *Polymer* **65** 215–22
[7] Babaahmadi M, Sabzi M, Mahdavinia G R and Keramati M 2017 Preparation of amorphous nanocomposites with quick heat triggered shape memory behavior *Polymer* **112** 26–34
[8] Xiao X, Kong D, Qiu X, Zhang W, Zhang F, Liu L, Liu Y, Zhang S, Hu Y and Leng J 2015 Shape-memory polymers with adjustable high glass transition temperatures *Macromolecules* **48** 3582–9
[9] Leng J, Huang W, Lan X, Liu Y and Du S 2008 Significantly reducing electrical resistivity by forming conductive Ni chains in a polyurethane shape-memory polymer/carbon-black composite *Appl. Phys. Lett.* **92** 204101
[10] Leng J, Lan X, Liu Y, Du S, Huang W, Liu N, Phee S and Yuan Q 2008 Electrical conductivity of thermoresponsive shape-memory polymer with embedded micron sized Ni powder chains *Appl. Phys. Lett.* **92** 014104
[11] Wei K, Zhu G, Tang Y and Li X 2013 Electroactive shape-memory effects of hydro-epoxy/carbon black composites *Polym. J.* **45** 671
[12] Luo H, Li Z, Yi G, Zu X, Wang H, Wang Y, Huang H, Hu J, Liang Z and Zhong B 2014 Electro-responsive silver nanowire-shape memory polymer composites *Mater. Lett.* **134** 172–5
[13] Liu T, Huang R, Qi X, Dong P and Fu Q 2017 Facile preparation of rapidly electro-active shape memory thermoplastic polyurethane/polylactide blends via phase morphology control and incorporation of conductive fillers *Polymer* **114** 28–35
[14] Mohr R, Kratz K, Weigel T, Lucka-Gabor M, Moneke M and Lendlein A 2006 Initiation of shape-memory effect by inductive heating of magnetic nanoparticles in thermoplastic polymers *Proc. Natl Acad. Sci.* **103** 3540–5
[15] Zhang F, Zhang Z, Luo C, Lin I T, Liu Y, Leng J and Smoukoy S K 2015 Remote, fast actuation of programmable multiple shape memory composites by magnetic fields *J. Mater. Chem.* C **3** 11290–3

[16] Maitland D J, Metzger M F, Schumann D, Lee A and Wilson T S 2002 Photothermal properties of shape memory polymer micro-actuators for treating stroke *Lasers Surg. Med.* **30** 1–11

[17] Small W IV, Wilson T S, Benett W J, Loge J M and Maitland D J 2005 Laser-activated shape memory polymer intravascular thrombectomy device *Opt. Express* **13** 8204–13

[18] Jiang H, Kelch S and Lendlein A 2006 Polymers move in response to light *Adv. Mater.* **18** 1471–5

[19] Lu H, Liu Y, Leng J and Du S 2009 Qualitative separation of the effect of the solubility parameter on the recovery behavior of shape-memory polymer *Smart Mater. Struct.* **18** 085003

[20] Yang B, Huang W, Li C, Lee C and Li L 2003 On the effects of moisture in a polyurethane shape memory polymer *Smart Mater. Struct.* **13** 191

[21] Huang W, Yang B, An L, Li C and Chan Y 2005 Water-driven programmable polyurethane shape memory polymer: demonstration and mechanism *Appl. Phys. Lett.* **86** 114105

[22] Yang B, Huang W, Li C and Li L 2006 Effects of moisture on the thermomechanical properties of a polyurethane shape memory polymer *Polymer* **47** 1348–56

[23] Lv H, Leng J, Liu Y and Du S 2008 Shape-memory polymer in response to solution *Adv. Eng. Mater.* **10** 592–5

[24] Fan J and Li G 2018 High enthalpy storage thermoset network with giant stress and energy output in rubbery state *Nat. Commun.* **9** 642

[25] Rousseau I A 2008 Challenges of shape memory polymers: a review of the progress toward overcoming SMP's limitations *Polym. Eng. Sci.* **48** 2075–89

[26] Wei Z, Sandstroröm R and Miyazaki S 1998 Shape-memory materials and hybrid composites for smart systems: I. Shape-memory materials *J. Mater. Sci.* **33** 3743–62

[27] http://www2.smptechno.com/en/tech/pdf/%5B2018%5DSMP%20Tech%20E-Catalogue.pdf

[28] Wei H, Liu L, Zhang Z, Du H, Liu Y and Leng J 2015 Design and analysis of smart release devices based on shape memory polymer composites *Compos. Struct.* **133** 642–51

[29] Ratna D and Karger-Kocsis J 2008 Recent advances in shape memory polymers and composites: a review *J. Mater. Sci.* **43** 254–69

[30] Kunzelman J, Chung T, Mather P T and Weder C 2008 Shape memory polymers with built-in threshold temperature sensors *J. Mater. Chem.* **18** 1082–6

[31] Mather P T, Luo X and Rousseau I A 2009 Shape memory polymer research *Annu. Rev. Mater. Res.* **39** 445–71

[32] Huang W, Ding Z, Wang C, Wei J, Zhao Y and Purnawali H 2010 Shape memory materials *Mater. Today* **13** 54–61

[33] Hu J, Zhu Y, Huang H and Lu J 2012 Recent advances in shape–memory polymers: Structure, mechanism, functionality, modeling and applications *Prog. Polym. Sci.* **37** 1720–63

[34] Jin X, Ni Q Q and Natsuki T 2011 Composites of multi-walled carbon nanotubes and shape memory polyurethane for electromagnetic interference shielding *J. Compos. Mater.* **45** 2547–54

[35] Ni Q Q, Zhang C S, Fu Y, Dai G and Kimura T 2007 Shape memory effect and mechanical properties of carbon nanotube/shape memory polymer nanocomposites *Compos. Struct.* **81** 176–84

[36] Yakacki C M, Satarkar N S, Gall K, Likos R and Hilt J Z 2009 Shape-memory polymer networks with Fe3O4 nanoparticles for remote activation *J. Appl. Polym. Sci.* **112** 3166–76

[37] Gall K, Dunn M L, Liu Y, Finch D, Lake M and Munshi N A 2002 Shape memory polymer nanocomposites *Acta Mater.* **50** 5115–26

[38] Liu T, Liu L, Yu M, Li Q, Zeng C, Lan X, Liu Y and Leng J 2018 Integrative hinge based on shape memory polymer composites: material, design, properties and application *Compos. Struct.* **206** 164–76

[39] Barrett R, Francis W, Abrahamson E, Lake M and Scherbarth M 2006 Qualification of elastic memory composite hinges for spaceflight applications *47th AIAA/ASME/ASCE/AHS/ASC Structures, Structural Dynamics, and Materials Conf. 14th AIAA/ASME/AHS Adaptive Structures Conf. 7th* 2039

[40] Herath H, Epaarachchi J A, Islam M M, Al-Azzawi W, Leng J and Zhang F 2018 Structural performance and photothermal recovery of carbon fibre reinforced shape memory polymer *Compos. Sci. Technol.* **167** 206–14

[41] Wei Z, Sandstrom R and Miyazaki S 1998 Shape memory materials and hybrid composites for smart systems: II. Shape-memory hybrid composites *J. Mater. Sci.* **33** 3763–83

[42] Hu J, Meng H, Li G and Ibekwe S I 2012 A review of stimuli-responsive polymers for smart textile applications *Smart Mater. Struct.* **21** 053001

[43] Chan Vili Y Y 2007 Investigating smart textiles based on shape memory materials *Text. Res. J.* **77** 290–300

[44] Mondal S and Hu J 2006 Temperature stimulating shape memory polyurethane for smart clothing *Indian J. Fibre Text. Res.* **31** 66–71

[45] Zhu Y, Hu J, Luo H, Young R J, Deng L, Zhang S, Fan Y and Ye G 2012 Rapidly switchable water-sensitive shape-memory cellulose/elastomer nano-composites *Soft Matter* **8** 2509–17

[46] Lee J H, Hinchet R, Kim S K, Kim S and Kim S-W 2015 Shape memory polymer-based self-healing triboelectric nanogenerator *Energy Environ. Sci.* **8** 3605–13

[47] Browne A L, Johnson N L and Namuduri C S 2005 Electrostatically releasable fastening system and method of use *US Patent* 6944920

[48] Browne A L and Johnson N L 2008 Hood assembly utilizing active materials based mechanisms *US Patent* 7392876

[49] Lendlein A, Behl M, Hiebl B and Wischke C 2010 Shape-memory polymers as a technology platform for biomedical applications *Expert Rev. Med. Devices* **7** 357–79

[50] Zhang R, Guo X, Liu Y and Leng J 2014 Theoretical analysis and experiments of a space deployable truss structure *Compos. Struct.* **112** 226–30

[51] Liu Y, Du H, Liu L and Leng J 2014 Shape memory polymers and their composites in aerospace applications: a review *Smart Mater. Struct.* **23** 023001

[52] Vernon L B and Vernon H M 1941 Process of manufacturing articles of thermoplastic synthetic resins *US Patent* 2234993

[53] Liu C, Qin H and Mather P 2007 Review of progress in shape-memory polymers *J. Mater. Chem.* **17** 1543–58

[54] Perrone R 1967 Heat-shrinkable articles made from silicone rubber–polyethylene compositions *US Pat.* 3326869

[55] Wray P 1967 Elastic memory articles *US Pat.* GB1075704

[56] Arditti S, Avedikian S and Bernstein B 1971 Articles with polymeric memory *US Pat.* 3563973

[57] Irie M 1998 *Shape Memory Polymers* (Cambridge: Cambridge University Press) pp 203–19

[58] Lendlein A and Kelch S 2002 Shape-memory polymers *Angew. Chem. Int. Ed.* **41** 2034–57

[59] Huang W, Yang B, Zhao Y and Ding Z 2010 Thermo-moisture responsive polyurethane shape-memory polymer and composites: a review *J. Mater. Chem.* **20** 3367–81

[60] Schmidt C, Chowdhury A M S, Neuking K and Eggeler G 2011 Mechanical behavior of shape memory polymers by 1WE method: application to Tecoflex® thermoplast *Compos. Mater.* **24** 853–60

[61] Everhart M C, Nickerson D M and Hreha R D 2006 High-temperature reusable shape memory polymer mandrels *Proc. SPIE 6171, Smart Structures and Materials 2006: Industrial*

and Commercial Applications of Smart Structures Technologies 61710K

[62] McClung A J, Tandon G P and Baur J W 2012 Strain rate-and temperature-dependent tensile properties of an epoxy-based, thermosetting, shape memory polymer (Veriflex-E) *Mech. Time-Depend. Mater.* **16** 205–21

[63] Gall K, Mikulas M, Munshi N A, Beavers F and Tupper M 2000 Carbon fiber reinforced shape memory polymer composites *J. Intell. Mater. Syst. Struct.* **11** 877–86

[64] Arzberger S C, Munshi N A, Lake M S, Wintergerst J, Varlese S and Ulmer M P 2003 Elastic memory composite technology for thin lightweight space-and ground-based deployable mirrors *Proc. SPIE, Optical Materials and Structures Technologies* **5179** 143–154

[65] Arzberger S C *et al* 2005 Elastic memory composites (EMC) for deployable industrial and commercial applications *Proc. SPIE 5762, Smart Structures and Materials 2005: Industrial and Commercial Applications of Smart Structures Technologies* **5762** 35–47

[66] Cadogan D, Scarborough S, Lin J and Sapna G H 2002 Shape memory composite development for use in Gossamer space inflatable structure *43rd AIAA/ASME/ASCE/AHS/ASC Structures, Structural Dynamics, and Materials Conf.* 1372

[67] Osada Y and Matsuda A 1995 Shape memory in hydrogels *Nature* **376** 219

[68] Hao J and Weiss R A 2013 Mechanically tough, thermally activated shape memory hydrogels *ACS Macro Lett.* **2** 86–9

[69] Mitsumata T, Gong J P and Osada Y 2001 Shape memory functions and motility of amphiphilic polymer gels *Polym. Adv. Technol.* **12** 136–50

[70] Santo L, Quadrini F, Squeo E A, Dolce F, Mascetti G, Bertolotto D, Villadei W, Ganga P L and Zolesi V 2012 Behavior of shape memory epoxy foams in microgravity: experimental results of STS-134 mission *Microgravity Sci. Technol.* **24** 287–96

[71] Santo L, Quadrini F, Ganga P L and Zolesi V 2015 Mission BION-M1: results of Ribes/Foam2 experiment on shape memory polymer foams and composites *Aerosp. Sci. Technol.* **40** 109–14

[72] Lendlein A, Schmidt A M and Langer R 2001 AB-polymer networks based on oligo (ε-caprolactone) segments showing shape-memory properties *Proc. Natl. Acad. Sci. U. S. A.* **98** 842–7

[73] Alteheld A, Feng Y, Kelch S and Lendlein A 2005 Biodegradable, amorphous copolyester-urethane networks having shape-memory properties *Angew. Chem. Int. Ed.* **44** 1188–92

[74] Lendlein A and Kelch S 2005 Shape-memory polymers as stimuli-sensitive implant materials *Clin. Hemorheol. Microcirc.* **32** 105–16

[75] Lendlein A, Schmidt A M, Schroeter M and Langer R 2005 Shape-memory polymer networks from oligo (ϵ-caprolactone) dimethacrylates *J. Polym. Sci.* A **43** 1369–81

[76] Ji F, Zhu Y, Hu J, Liu Y, Yeung L Y and Ye G 2006 Smart polymer fibers with shape memory effect *Smart Mater. Struct.* **15** 1547

[77] Meng Q, Liu J, Shen L, Hu Y and Han J 2009 A smart hollow filament with thermal sensitive internal diameter *J. Appl. Polym. Sci.* **113** 2440–9

[78] Hu J and Chen S 2010 A review of actively moving polymers in textile applications *J. Mater. Chem.* **20** 3346–55

[79] Xie F, Huang L, Liu Y and Leng J 2012 Modified shape memory cyanate polymers with a wide range of high glass transition temperatures *Proc. SPIE 8342, Behavior and Mechanics of Multifunctional Materials and Composites* 834210

[80] Lan X, Liu Y, Lv H, Wang X, Leng J and Du S 2009 Fiber reinforced shape-memory polymer composite and its application in a deployable hinge *Smart Mater. Struct.* **18** 024002

[81] Leng J, Wu X and Liu Y 2009 Effect of a linear monomer on the thermomechanical properties of epoxy shape-memory polymer *Smart Mater. Struct.* **18** 095031

[82] Li F, Liu L, Lan X, Zhou X, Bian W, Liu Y and Leng J 2016 Preliminary design and analysis of a cubic deployable support structure based on shape memory polymer composite *Int. J. Smart Nano Mater.* **7** 106–18

[83] Lake M, Munshi N, Meink T, Tupper M and Meink T 2001 Application of elastic memory composite materials to deployable space structures *AIAA Space 2001 Conf. and Exposition* 4602

[84] Behl M, Razzaq M Y and Lendlein A 2010 Multifunctional shape-memory polymers *Adv. Mater.* **22** 3388–410

[85] Meng Q and Hu J 2009 A review of shape memory polymer composites and blends *Composites* A **40** 1661–72

[86] Mu T, Liu L, Lan X, Liu Y and Leng J 2018 Shape memory polymers for composites *Compos. Sci. Technol.* **160** 169–98

[87] Rubinstein M and Colby R H 2003 *Polymer Physics* (New York: Oxford University Press)

[88] Liu C, Chun S B, Mather P T, Zheng L, Haley E H and Coughlin E B 2002 Chemically cross-linked polycyclooctene: synthesis, characterization, and shape memory behavior *Macromolecules* **35** 9868–74

[89] Zhang S, Feng Y, Zhang L, Sun J, Xu X and Xu Y 2007 Novel interpenetrating networks with shape-memory properties *Polym. Sci.* A **45** 768–75

[90] Tang Y, Jiang Z, Men Y, An L, Enderle H-F, Lilge D, Roth S V, Gehrke R and Rieger J 2007 Uniaxial deformation of overstretched polyethylene: *in situ* synchrotron small angle x-ray scattering study *Polymer* **48** 5125–32

[91] Kolesov I, Dolynchuk O, Jehnichen D, Reuter U, Stamm M and Radusch H-J 2015 Changes of crystal structure and morphology during two-way shape-memory cycles in cross-linked linear and short-chain branched polyethylenes *Macromolecules* **48** 4438–50

[92] Wang W, Jin Y, Ping P, Chen X, Jing X and Su Z 2010 Structure evolution in segmented poly (ester urethane) in shape-memory process *Macromolecules* **43** 2942–7

[93] Hoeher R, Raidt T, Krumm C, Meuris M, Katzenberg F and Tiller J C 2013 Tunable multiple-shape memory polyethylene blends *Macromol. Chem. Phys.* **214** 2725–1732

[94] Zhao Q, Qi H and Xie T 2015 Recent progress in shape memory polymer: new behavior, enabling materials, and mechanistic understanding *Prog. Polym. Sci.* **49** 79–120

[95] Gu J, Sun H and Fang C 2014 A multi-branch finite deformation constitutive model for a shape memory polymer based syntactic foam *Smart Mater. Struct.* **24** 025011

[96] Tobushi H, Hashimoto T, Hayashi S and Yamada E 1997 Thermomechanical constitutive modeling in shape memory polymer of polyurethane series *J. Intell. Mater. Syst. Struct.* **8** 711–8

[97] Tobushi H, Okumura K, Hayashi S and Norimitsu I 2001 Thermomechanical constitutive model of shape memory polymer *Mech. Mater.* **33** 545–54

[98] Nguyen T, Qi H, Castro F and Long K 2008 A thermoviscoelastic model for amorphous shape memory polymers: incorporating structural and stress relaxation *J. Mech. Phys. Solids* **56** 2792–814

[99] Gu J, Leng J and Sun H 2017 A constitutive model for amorphous shape memory polymers based on thermodynamics with internal state variables *Mech. Mater.* **111** 1–14

[100] Liu Y, Gall K, Dunn M L, Greenberg A R and Diani J 2006 Thermomechanics of shape memory polymers: uniaxial experiments and constitutive modeling *Int. J. Plast.* **22** 279–313

[101] Chen Y and Lagoudas D C 2008 A constitutive theory for shape memory polymers: I. Large deformations *J. Mech. Phys. Solids* **56** 1752–65
[102] Chen Y and Lagoudas D C 2008 A constitutive theory for shape memory polymers. Part II: A linearized model for small deformations *J. Mech. Phys. Solids* **56** 1766–78
[103] Guo X, Liu L, Zhou B, Liu Y and Leng J 2016 Constitutive model for shape memory polymer based on the viscoelasticity and phase transition theories *J. Intell. Mater. Syst. Struct.* **27** 314–23
[104] Park H, Harrison P, Guo Z, Lee M and Yu W 2016 Three-dimensional constitutive model for shape memory polymers using multiplicative decomposition of the deformation gradient and shape memory strains *Mech. Mater.* **93** 43–62
[105] Li Y and Liu Z 2018 A novel constitutive model of shape memory polymers combining phase transition and viscoelasticity *Polym.* **143** 298–308
[106] Ni Q-Q, Zhang R-X, Natsuki T and Iwamoto M 2007 Stiffness and vibration characteristics of SMA/ER3 composites with shape memory alloy short fibers *Compos. Struct.* **79** 501–7
[107] Liu Y, Han C, Tan H and Du X 2010 Thermal, mechanical and shape memory properties of shape memory epoxy resin *Mater. Sci. Eng.* A **527** 2510–4
[108] Li X, Zhu Y, Dong Y, Liu M, Ni Q and Fu Y 2015 Epoxy resin composite bilayers with triple-shape memory effect *J. Nanomater.* **2015** 2
[109] Gall K, Dunn M L, Liu Y, Finch D, Lake M and Munshi N A 2002 Shape memory polymer nanocomposites *Acta Mater.* **50** 5115–26
[110] Dong Y and Ni Q Q 2015 Effect of vapor-grown carbon nanofibers and *in situ* hydrolyzed silica on the mechanical and shape memory properties of water-borne epoxy composites *Polym. Compos.* **36** 1712–20
[111] Ramani T 2017 Thermo-mechanical characterization of carbon-reinforced shape memory polymer *Dissertation for the Doctoral Degree in Engineering USA* University of Illinois at Urbana-Champaign
[112] Robinson P, Bismarck A, Zhang B and Maples H A 2017 Deployable, shape memory carbon fibre composites without shape memory constituents *Compos. Sci. Technol.* **145** 96–104
[113] Lan X, Liu L, Liu Y, Leng J and Du S 2014 Post microbuckling mechanics of fibre-reinforced shape-memory polymers undergoing flexure deformation *Mech. Mater.* **72** 46–60
[114] Thompson J M T and Hunt G W 1973 *A General Theory of Elastic Stability J.* (London: Wiley)
[115] Francis W, Lake M, Schultz M, Campbell D, Dunn M and Qi H J 2007 Elastic memory composite microbuckling mechanics: closed-form model with empirical correlation *48th AIAA/ASME/ASCE/AHS/ASC Structures, Structural Dynamics, and Materials Conf. (April2164*
[116] Gall K, Mikulas M, Tupper M, Munshi N and Mikulas M 2001 Micro-mechanisms of deformation in fiber reinforced polymer matrix elastic memory composites *19th AIAA Applied Aerodynamics Conf.* 1419
[117] Murphey T, Meink T and Mikulas M 2001 Some micromechanics considerations of the folding of rigidizable composite materials *19th AIAA Applied Aerodynamics Conf.* 1418
[118] Zhang J, Dui G and Liang X 2018 Revisiting the micro-buckling of carbon fibers in elastic memory composite plates under pure bending *Int. J. Mech. Sci.* **136** 339–48
[119] Tan Q, Liu L, Liu Y and Leng J 2014 Thermal mechanical constitutive model of fiber reinforced shape memory polymer composite: based on bridging model *Composites* A **64** 132–8
[120] Roh J, Kim H and Bae J 2014 Shape memory polymer composites with woven fabric reinforcement for self-deployable booms *J. Intell. Mater. Syst. Struct.* **25** 2256–66
[121] Gu J, Leng J, Sun H, Zeng H and Cai Z 2019 Thermomechanical constitutive modeling of fiber reinforced shape memory polymer composites based on thermodynamics with internal state variables *Mech. Mater.* **130** 9–19
[122] Kern K T, Stancil P C, Harries W L, Long E R Jr and Thibeault S A 1993 Simulated space environmental effects on a polyetherimide and its carbon fiber-reinforced composites *SAMPE J.* **29** 29–44
[123] Hossain U and Ensinger W 2015 Experimental simulation of radiation damage of polymers in space applications by cosmic-ray-type high energy heavy ions and the resulting changes in optical properties *Nucl. Instrum. Methods Phys. Res.,* B **365** 230–4
[124] Scott G 1990 *Mechanisms of Polymer Degradation and Stabilisation* (London: Elsevier Applied Science)
[125] Skurat V, Barbashev E, Dorofeev Y I, Nikiforov A, Gorelova M and Pertsyn A 1996 Simulation of polymer film and surface behaviour in a space environment *Appl. Surf. Sci.* **92** 441–6
[126] Paillous A and Pailler C 1994 Degradation of multiply polymer-matrix composites induced by space environment *Composites* **25** 287–95
[127] Han J H and Kim C G 2006 Low earth orbit space environment simulation and its effects on graphite/epoxy composites *Compos. Struct.* **72** 218–26
[128] Silverman E M 1995 Space environmental effects on spacecraft: LEO materials selection guide *NASA Contractor Report 4661* part 1 (https://ntrs.nasa.gov/archive/nasa/casi.ntrs.nasa.gov/19960000860.pdf)
[129] Dever J, Miller S, Messer R, Sechkar E and Tollis G 2001 Exposure of polymer film thermal control materials on the materials international space station experiment (MISSE) *2001 Conference and Exhibit on International Space Station Utilization* 4924
[130] Srinivasan V and Banks B A 1990 Materials degradation in low earth orbit (LEO) *Proc. Symp., 119th Annual Meeting of the Minerals, Metals, and Materials Society* 17–22
[131] Leger L and Bricker R W 1972 Apollo Experience Report Window Contamination *NASA Technical Note* NASA TN D-6721
[132] Barnes J and Cogswell F 1989 Thermoplastics for space *SAMPE Q.* **20** 22–7
[133] ASTM E595-15 2015 *Standard test Method for Total Mass Loss and Collected Volatile Condensable Materials from Outgassing in a Vacuum Environment West Conshohocken* (PA: ASTM International)
[134] Pagano N, Schoeppner G, Kim R and Abrams F 1998 Steady-state cracking and edge effects in thermo-mechanical transverse cracking of cross-ply laminates *Compos. Sci. Technol.* **58** 1811–25
[135] Hancox N 1998 Thermal effects on polymer matrix composites: Part 1. Thermal cycling *Mater. Des.* **19** 85–91
[136] Shin K B, Kim C G, Hong C S and Lee H H 2001 Thermal distortion analysis of orbiting solar array including degradation effects of composite materials *Composites* B **32** 271–85
[137] Bianchi J and Jang B 1995 Evaluation of epoxy matrix composites exposed to atomic oxygen *J. Adv. Mater.* **26** 10–7
[138] Tennyson R C 1991 Atomic oxygen effects on polymer-based materials *Can. J. Phys.* **69** 1190–208
[139] Liau W and Tseng F 1998 The effect of long-term ultraviolet light irradiation on polymer matrix composites *Polym. Compos.* **19** 440–5

[140] Banks B A, de Groh K K and Miller S K 2004 Low earth orbital atomic oxygen interactions with spacecraft materials *MRS Online Proc. Libr.* **851** NN8.1

[141] Arnold G S and Peplinksi D 1986 Reaction of high-velocity atomic oxygen with carbon *AIAA J.* **24** 673–7

[142] Xie F, Liu L, Gong X, Huang L, Leng J and Liu Y 2017 Effects of accelerated aging on thermal, mechanical and shape memory properties of cyanate-based shape memory polymer: I vacuum ultraviolet radiation *Polym. Degrad. Stab.* **138** 91–7

[143] Tan Q, Li F, Liu L, Chu H, Liu Y and Leng J 2018 Effects of atomic oxygen on epoxy-based shape memory polymer in low earth orbit *J. Intell. Mater. Syst. Struct.* **29** 1081–7

[144] Nambiar S and Yeow J T W 2012 Polymer-composite materials for radiation protection *ACS Appl. Mater. Interfaces* **4** 5717–26

[145] Gao H, Lan X, Liu L, Xiao X, Liu Y and Leng J 2017 Study on performances of colorless and transparent shape memory polyimide film in space thermal cycling, atomic oxygen and ultraviolet irradiation environments *Smart Mater. Struct.* **26** 095001

[146] Xie F, Huang L, Leng J and Liu Y 2016 Thermoset shape memory polymers and their composites *J. Intell. Mater. Syst. Struct.* **27** 2433–55

[147] Tompkins S, Bowles D, Slemp W and Teichman L 1988 Response of composite materials to the space station orbit environment *29th Structures, Structural Dynamics and Materials Conf.* 2476

[148] Dever J, Pietromica A, Stueber T, Sechkar E and Messer R 2001 Simulated space vacuum ultraviolet (VUV) exposure testing for polymer films *39th Aerospace Sciences Meeting and Exhibit* 1054

[149] Dever J, McCracken C and Bruckner E 2004 Vacuum ultraviolet radiation characterization of RF air plasma and effects on polymer films *Protection of Materials and Structures from Space Environment* (Dordrecht: Springer) 335–50

[150] Trick K A and Saliba T E 1995 Mechanisms of the pyrolysis of phenolic resin in a carbon/phenolic composite *Carbon* **3** 1509–15

[151] Chang C and Tackett J R 1991 Characterization of phenolic resins with thermogravimetry-mass spectrometry *Thermochim. Acta* **192** 181–90

[152] https://directory.eoportal.org/web/eoportal/satellite-missions/t/tacsat-2

[153] https://www.nasa.gov/mission_pages/station/research/experiments/explorer/Investigation.html?#id=53

[154] Keller P, Lake M, Francis W, Harvey J, Ruhl E, Winter J, Scherbarth M R and Murphey T W 2004 Development of a deployable boom for microsatellites using elastic memory composite material *45th AIAA/ASME/ASCE/AHS/ASC Structures, Structural Dynamics & Materials Conf. (April (Palm Springs, California, USA) p 1603*

[155] https://directory.eoportal.org/web/eoportal/satellite-missions/f/falconsat-3

[156] Aoki T, Higuchi K and Watanabe K 2014 Progress Report of SIMPLE Space Experiment Project on ISS Japan Experiment Module *TRANSACTIONS OF THE JAPAN SOCIETY FOR AERONAUTICAL AND SPACE SCIENCES, AEROSPACE TECHNOLOGY JAPAN* **12** Tc_1-Tc_6

[157] Li F, Liu L, Lan X, Pan C, Liu Y, Leng J and Xie Q 2019 Ground and geostationary orbital qualification of a sunlight-stimulated substrate based on shape memory polymer composite *Smart Mater. Struct.* **28** 075023

[158] Dao T D, Ha N S, Goo N S and Yu W R 2018 Design, fabrication, and bending test of shape memory polymer composite hinges for space deployable structures *J. Intell. Mater. Syst. Struct.* **29** 1560–74

[159] Taylor R, Abrahamson E, Barrett R, Codell D and Keller P 2007 Passive deployment of an emc boom using radiant energy in thermal vacuum *48th AIAA/ASME/ASCE/AHS/ASC Structures, Structural Dynamics, and Materials Conf.* 2269

[160] Francis W, Lake M, Peterson L and Hinkle J 2004 Development of an elastic memory composite self-locking linear actuator for deployable optics *45th AIAA/ASME/ASCE/AHS/ASC Structures, Structural Dynamics & Materials Conf.* 1821

[161] Keller P, Lake M, Codell D, Barrett R, Taylor R and Schultz M 2006 Development of elastic memory composite stiffeners for a flexible precision reflector *47th AIAA/ASME/ASCE/AHS/ASC Structures, Structural Dynamics, and Materials Conf. 14th AIAA/ASME/AHS Adaptive Structures Conf. 7th* 2179

[162] Chen Q, Yao Z, Hou Y and Fang H 2017 Design and testing of a space deployable mechanism *4th AIAA Spacecraft Structures Conf.* 0176

[163] Senba A, Ogi Y and Kogiso N 2013 Wrinkle/slack control using shape memory polymer films for large membrane structures *54th AIAA/ASME/ASCE/AHS/ASC Structures, Structural Dynamics, and Materials Conf.* 1928

[164] Rakow A, Hedin K and Anthony B 2018 *Development of High Specific Power Solar Arrays with Shape Memory Polymer Hinge Lines AIAA Spacecraft Structures Conf.* 2206

[165] Li F, Liu L, Lan X, Wang T, Li X, Chen F, Bian W, Liu Y and Leng J 2016 Modal analyses of deployable truss structures based on shape memory polymer composites *Int. J. Appl. Mech.* **8** 1640009

[166] Santo L, Quadrini F and Bellisario D 2016 Shape memory composite antennas for space applications *IOP Conf. Ser.: Mater. Sci. Eng.* **161** 012066

[167] Dearborn M E, Andersen G P, Asmolova O, Balthazor R L, McHarg M G, Nelson H C, Quiller T S, Wilson G R, Harvey T J and Murphey T W 2014 A deployable membrane telescope payload for cubesats *JoSS* **3** 253–64

[168] Chen T, Bilal O R, Lang R, Daraio C and Shea K 2019 Autonomous deployment of a solar panel using an elastic origami and distributed shape memory polymer actuators *Phys. Rev. Appl.* **11** 064069

[169] Kang T H, Lee J M, Yu W R, Youk J H and Ryu H W 2012 Two-way actuation behavior of shape memory polymer/elastomer core/shell composites *Smart Mater. Struct.* **21** 035028

[170] Lu L and Li G 2016 One-way multishape-memory effect and tunable two-way shape memory effect of ionomer poly (ethylene-co-methacrylic acid) *ACS Appl. Mater. Interfaces* **8** 14812–23

[171] Lu L, Cao J and Li G 2018 Giant reversible elongation upon cooling and contraction upon heating for a crosslinked cis poly(1, 4-butadiene) system at temperatures below zero Celsius *Sci. Rep.* **8** 14233